Reliability Engineering and System Safety 270 (2026) 112155

Contents lists available at ScienceDirect

Reliability Engineering and System Safety

journal homepage: www.elsevier.com/locate/ress

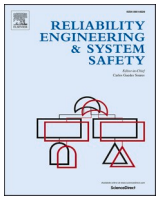

Vulnerability of process and instrument air supply utilities to volcanic ash

Matteo Valente, Federica Ricci *, Valerio Cozzani

LISES - Laboratory of Industrial Safety and Environmental Sustainability, Department of Civil, Chemical, Environmental, and Material Engineering, University of Bologna, via Terracini 28, Bologna 40131, Italy

ARTICLE INFO

Keywords:
Natech
Volcanic ash
Filtration system
Time to clogging
Volcanic hazard
Vulnerability matrix

ABSTRACT

Among other consequences of volcanic activity, recent events confirmed that the hazards caused by volcanic ash have a potential impact also at relevant distances from the emission point. The fallout of volcanic ashes may affect several utilities and services at industrial sites, potentially causing Natech events with relevant end-point consequences, e.g., operational failures, business interruption, and environmental contamination. The present study focuses on the vulnerability of process and instrument air intake utility systems to volcanic ash. A detailed model, based on an in-depth characterization of ash properties, is developed to provide accurate time to clogging estimations under varying conditions. A surrogate model is also proposed to enable a real-time assessment using a limited set of input parameters, supporting both preventive planning and real-time decision-making in emergency management. A tailored risk matrix is developed to provide a scenario-specific vulnerability ranking of critical utilities due to volcanic ash accumulation. A novel quantitative approach for the assessment of risk due to filter clogging has also been developed to support the management of the vulnerabilities and critical scenarios identified by the matrix screening. The analysis of test cases confirmed the value of the novel approach in supporting risk management and resilience against volcanic hazards, aimed at the mitigation of operational disruptions and/or more severe process safety accidents.

1. Introduction

Technological accidents triggered by the impact of natural hazards (Natech accidents) represent a relevant category of cascading events affecting several industrial activities [1,2] and causing prolonged downtime of impacted facilities [3,4]. Many industrial installations are not designed to withstand Natech events, and natural hazards may trigger unexpected accident scenarios unlikely to take place in the case of conventional causes [5]. These scenarios can occur not only as a result of high-intensity natural disasters, but low-intensity natural hazards are increasingly being recognized as causes of accidents as well [6–8]. In recent years, the increasing frequency and intensity of extreme natural events due to climate change [9] exacerbated the occurrence and severity of Natech accidents [10], highlighting the need to develop a systematic approach to assess this category of accidents. Significant progress has been made for "direct" Natech accidents, involving the loss of containment of hazardous substances caused by the structural damage of equipment items [11–13], also incorporating hazard-specific approaches to improve predictive accuracy [14]. Methodologies are now available to address Natech events due to earthquakes [15–17], floods [18,19], and other natural hazards such as strong winds [20] and winter storms [21]. However, “indirect” Natech events caused by the failure of site utilities, services, and safety barriers due to the impact of natural hazards are of particular concern [5,22]. Examples of such scenarios are the Arkema [23] and the Fukushima power station [24] accidents. In spite of the severity of such events, limited attention has been dedicated to date to assessing the hazards deriving from the failure of site utilities, e.g., cooling or heating services, instrument air, purging gases, and electric power supply, as a consequence of natural hazards [25,26].

The relevance of volcanic hazards for industrial installations is highlighted by the International Atomic Energy Agency (IAEA), which provides specific guidelines for the hazard assessments in nuclear installations [27,28]. For the most severe impact phenomena of volcanic hazards (e.g., lava flow and domes, pyroclastic density currents, debris avalanches, volcano-generated missiles, laharic flows), current practice and technical standards designate extended exclusion zones where industrial siting is not recommended. However, the application of safety criteria based on exclusion distances is not feasible when considering tephra fallout. Tephra is composed of volcanic fragments that range in size from blocks and bombs (diameters higher than 64 mm), lapilli (from 2 to 64 mm), and ash (lower than 2 mm). The fallout of the coarser

* Corresponding author.
E-mail address: federica.ricci18@unibo.it (F. Ricci).

https://doi.org/10.1016/j.ress.2025.112155
Received 29 April 2025; Received in revised form 18 December 2025; Accepted 23 December 2025
Available online 24 December 2025

Nomenclature

A	Intake area, m^2
a_i	Coefficients in the best-fit correlation of θ calculation, -
AM_{GSA}	Absolute mean sensitivity index, -
b_i	Coefficients in the best-fit correlation of θ calculation, -
C	Concentration in air, kg • m^{-3}
d_p	Mean particle size/diameter, m
e	Void fraction of the cake, -
E	Filtering efficiency, -
E_{PM10}	Filtration efficiency of particles with diameters lower than or equal to 10 μm, %
$E_{PM>50}$	Filtration efficiency of particles with diameters greater than or equal to 50 μm, %
$iter$	Generic iteration in the Monte Carlo simulation, -
l	Thickness of the cake, m
l_c	Maximum cake thickness, m
m_c	Mass of volcanic ash that leads to the critical pressure drops, kg
N_{iter}	Total number of iterations in the Monte Carlo simulation, -
P_{clog}	Deterministic clogging probability, -
$\bar{P}_{clog}$	Probabilistic clogging probability, -
S	Filtering area, m^2
SD_{GSA}	Standard deviation sensitivity index, -
σ_p	Grain size distribution, -
t	Generic time in Monte Carlo simulation, s
t_0	Initial time at which the volcanic ash reaches the area of interestInitial time in which the volcanic ash reaches the area of interest, s
t_{ESD}	Time for process shutdown completion, h
t_{max}	Maximum time considered in the Monte Carlo simulation, s
t_{PSD}	Time for process shutdown completion, h
T	Air temperature, K
ttc	Time to clogging, s
ttc_L	Time to clogging considering a loosely packing condition, s
ttc_T	Time to clogging considering a tapped packing condition, s
u	Inlet velocity of the intake air, m • s^{-1}
α_i	Coefficients in the best-fit correlation for void fraction (e) calculation, -
ΔP	Pressure drops, Pa
ΔP_i	Initial pressure drops, Pa
ΔP_{max}	Maximum allowable pressure drops, Pa
Δt	Time step in the Monte Carlo simulation, s
θ	Correlation parameter in the time to clogging calculation, s • kg • m^{-3} • Pa^{-1}
μ_f	Viscosity of the fluid, Pa • s
ρ_f	Density of the fluid, kg • m^{-3}
ρ_p	Mean density of the particles, kg • m^{-3}
ψ	Particle sphericity, -

Acronyms

DM	Detailed Model
ESD	Emergency shutdown
GSA	Global Sensitivity Analysis
LSA	Local Sensitivity Analysis
MC	Monte Carlo
PSD	Process shutdown
SM	Surrogate Model
VAAC	Volcanic Ash Advisory Center
VAE	Volcanic Ash Exposure
VAI	Volcanic Ash Impact
VVI	Volcanic ash Vulnerability Index

tephra components is generally confined to proximal areas around the vent [29,30]. Differently, the atmospheric dispersion and deposition of volcanic ash - composed of the finest particles - may affect much wider areas, in some cases extending to hundreds to even thousands of kilometers from the eruption source [30,31], as experienced in recent events that significantly disrupted aviation traffic [32,33]. For this reason, the direct structural damage potentially caused by volcanic ash in industrial and nuclear facilities has been addressed in several previous studies [27,28,34–37]. Several potential indirect scenarios caused by ash-induced failure of utilities were also identified (e.g., the disruption of electrical generators and transmission facilities causing power outages [38], the clogging of drains [39], the clogging of filters [40]), but less attention has been dedicated to date to the quantitative assessment of the associated risk.

The clogging of filtration systems for process and instrument air supply due to volcanic ash represents a particular concern, and it is widely documented as a key impact mechanism for critical infrastructure [41,42]. Filter clogging may also be associated to high-consequence accident scenarios, requiring the implementation of specific safety measures in sites exposed to the hazard [43,44]. When filters are installed on instrument air supply, the blockage may compromise the availability of process control systems relying on pneumatic remote actuation of valves and may affect operational safety, potentially causing indirect Natech scenarios. Considering filters on process air supply (e.g., in combustion systems or in air separation facilities), clogging may force to emergency shutdown, leading to production outage and potentially unsafe conditions. The system downtime may be prolonged due to delays in clean-up and replacement activities, which may be further hindered by the disruptions of external critical infrastructures (e.g., transportation, power supply, water systems [29,41]) caused by the volcanic ash fallout. As an example, extensive power outages were caused due to the clogging of air intakes at two thermal generation facilities during the 2011 Cordón Caulle volcanic complex eruption [45]. Since timely operations may mitigate such risk, effective management of the hazard due to these indirect Natech events is crucially dependent on the assessment of the time to clogging (*ttc*) of the filtration systems when exposed to volcanic ash, which in turn depends on the specific parameters of the fallout scenario and on the filtration system. However, in most previous studies, only qualitative or highly empirical semi-quantitative approaches were proposed to assess such hazards [34,46,47].

The present study focuses on the vulnerability to indirect Natech events triggered by the clogging of filtration systems due to volcanic ash deposition. A specific original model is developed to assess the time to clogging (*ttc*) of industrial filtration systems exposed to volcanic ash. The model is based on an in-depth characterization of ash properties to provide an accurate assessment of the time to clogging under different scenarios. The detailed model has been used to train a surrogate model allowing for a rapid and practical estimation of *ttc* using only a limited set of ash parameters. The *ttc* provides a key quantitative metric for evaluating the vulnerability of filtration systems to volcanic ash, thereby addressing the hazard associated with potential cascading Natech events deriving from the unavailability of instrument and/or process air. Based on the calculated *ttc* value, a matrix approach is proposed to evaluate a scenario-specific preliminary screening of the vulnerability due to volcanic ashes. A novel model to quantify the risk associated to the clogging of filter systems has also been developed, addressing the assessment of critical vulnerabilities identified by the screening matrix, thus providing a tool to support decision-making and to improve operational safety in facing volcanic hazards.

The paper is organized as follows: Section 2 describes the methodological approach developed. Two test cases are presented in Section 3.

Section 4 reports the results of test beds, focusing on the impact of volcanic ash parameters on the time to clogging. In Section 5 a discussion of the results is provided, also addressing the applicability of the proposed methodology to real-time hazard assessment. In Section 6 some conclusions are drawn.

2. Methodology

2.1. Modeling approach

The clogging of an industrial filtration system caused by the intake of volcanic ashes dispersed in the air is schematically represented in Fig. 1. Volcanic ashes enter the filtration system with the intake flow and are separated from the air by the filter panel. Then, the accumulation of the volcanic ash forms a cake on the panel that introduces an additional resistance to the airflow through the filter. Therefore, when the filtration system approaches its operating limit, indicated by a threshold pressure drop across its surface, it becomes susceptible to clogging, resulting in a significant reduction or complete blockage of the airflow through the system. Thus, the time to clogging, *ttc*, of filtration systems due to the accumulation of volcanic ash is defined as the time at which the pressure drops across the filter exceed the maximum allowable value.

Based on the schematization shown in Fig. 1, a novel approach was developed to assess the *ttc* and the related hazard due to potential cascading events. Fig. 2 shows the modeling approach applied and the flowchart of the methodology.

In the first step of the approach, data concerning the reference volcanic ash fallout scenarios, the air intake, and the industrial filtration systems considered were retrieved from the literature and the current industrial practice. In the second step of the approach, the *ttc* is calculated using a specifically developed detailed model. As shown in Fig. 2, the detailed model was also used to derive a surrogate model, providing a rapid estimate of the *ttc* based on limited data concerning the volcanic ash properties. In the third step of the methodology (see Fig. 2), an approach was developed to assess the scenario-specific vulnerability to cascading events, based on the comparison of the *ttc* to reference values available for the duration of the volcanic exposure and for the time required for process and emergency shutdown. Finally, in the last step of the methodology (Step 4 in Fig. 2) a Monte Carlo procedure may be applied to quantify the risk based on the clogging probability of vulnerable equipment identified by the screening matrix, thus enabling the quantitative assessment of critical vulnerabilities for the industrial site.

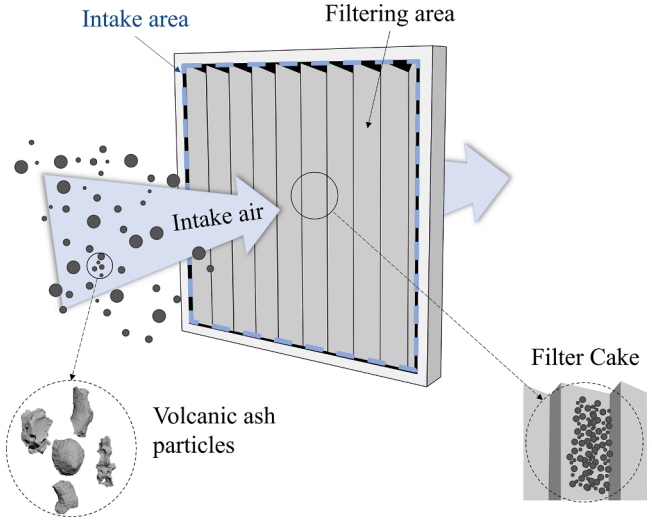

Fig. 1. Schematization of the phenomena leading to filter clogging due to the intake of volcanic ash in industrial filtration systems.

2.2. Step 1: input data collection

As shown in Fig. 2, the first part of the approach addresses the identification and collection of the necessary input data required to assess the *ttc* of an air filter in the presence of volcanic ash. Table 1 reports the list of input parameters necessary for applying the methodology developed in the present study. Specifically, parameters required for the time to clogging assessment relate to the characterization of intake air, volcanic ash, and the filtration system. A relevant issue related to the evaluation of time to clogging of filtering systems concerns the high variability and uncertainty of part of the parameters involved in the calculation. More specifically, all the parameters characterizing the volcanic ash concentration and size distribution exhibit both high time variability and uncertainty. Indeed, these parameters strongly depend on the specific volcanic event of concern, on the distance from the volcano, on meteorological conditions, and on the time since the start of the eruption. It should also be remarked that these parameters are also affected by epistemic uncertainty concerning the features of the emitted ash particles, due to the complex nature of volcanic scenarios.

It should also be highlighted that, as shown in Table 1, specific detailed input data are required to evaluate the volcanic ash vulnerability index used to assess the potential hazard for cascading Natech events: the estimated exposure time to the volcanic ash (intended as the foreseen duration of the presence of ash particles in the air intake), the time required to complete process shutdown (i.e., the normal shutdown procedure carried out to allow maintenance operations), and the time to complete emergency shutdown (i.e., the rapid shutdown caused by the presence of unsafe operating conditions).

2.3. Step 2: calculation of time to clogging

As shown in Fig. 2, the second step of the approach consists of the application of a model specifically developed to calculate the *ttc* of the filter due to the presence of volcanic ashes in the air intake. The model is based on the assessment of the additional pressure drops caused by the formation of a "cake" of ash particles. The time to clogging is estimated by calculating the time required for the additional pressure drops to reach the maximum allowable value derived from the design parameters of the blower used for the suction of the air intake.

2.3.1. Evaluation of additional pressure drops

The first step of the detailed model evaluates the additional pressure drops across the filter system due to the volcanic ash deposition. The Ergun correlation [48] was adopted to calculate the pressure drops:

$$-\frac{\Delta P}{l} = 150 \cdot \frac{(1-e)^2}{e^3} \cdot \frac{\mu_f \cdot u}{{d_p}^2} + 1.75 \cdot \frac{(1-e)}{e^3} \cdot \frac{\rho_f \cdot u^2}{d_p} \quad (1)$$

where ΔP is the pressure drop [Pa], l is the thickness of the cake [m], e is the void fraction of the cake [-], μ_f [Pa•s] and ρ_f [kg/m^3] are viscosity and density of air respectively, d_p is the mean particle size [m], and u is the inlet velocity of the intake air [m/s].

The application of the Ergun correlation requires the estimation of the void fraction of the cake, which can be evaluated using the semi-empirical correlation developed by Hoffmann and Finkers [49] as reported in Eq. (2):

$$e = 1 - \left\{1 - \left[(1-\alpha_1)\cdot\exp\left(\alpha_2 \cdot \rho_p \cdot d_p\right) + \alpha_1\right]\cdot\exp\left(\alpha_3 \cdot \sigma_p\right)\right\}\cdot\psi^{\alpha_4} \quad (2)$$

where d_p is the mean particle size [μm], ρ_p is the mean density of the particles [kg/m^3], σ is the grain size distribution [-], and ψ is the particle sphericity [-], whereas α_1, α_2, α_3, and α_4 are best-fitting parameters [-] derived from experimental data on void fractions and particle properties. Hoffmann and Finkers [49] proposed two sets of parameters, reported in Table 2, depending on the extent to which the bed packing is compressed. Actually, the void fraction (and therefore the specific

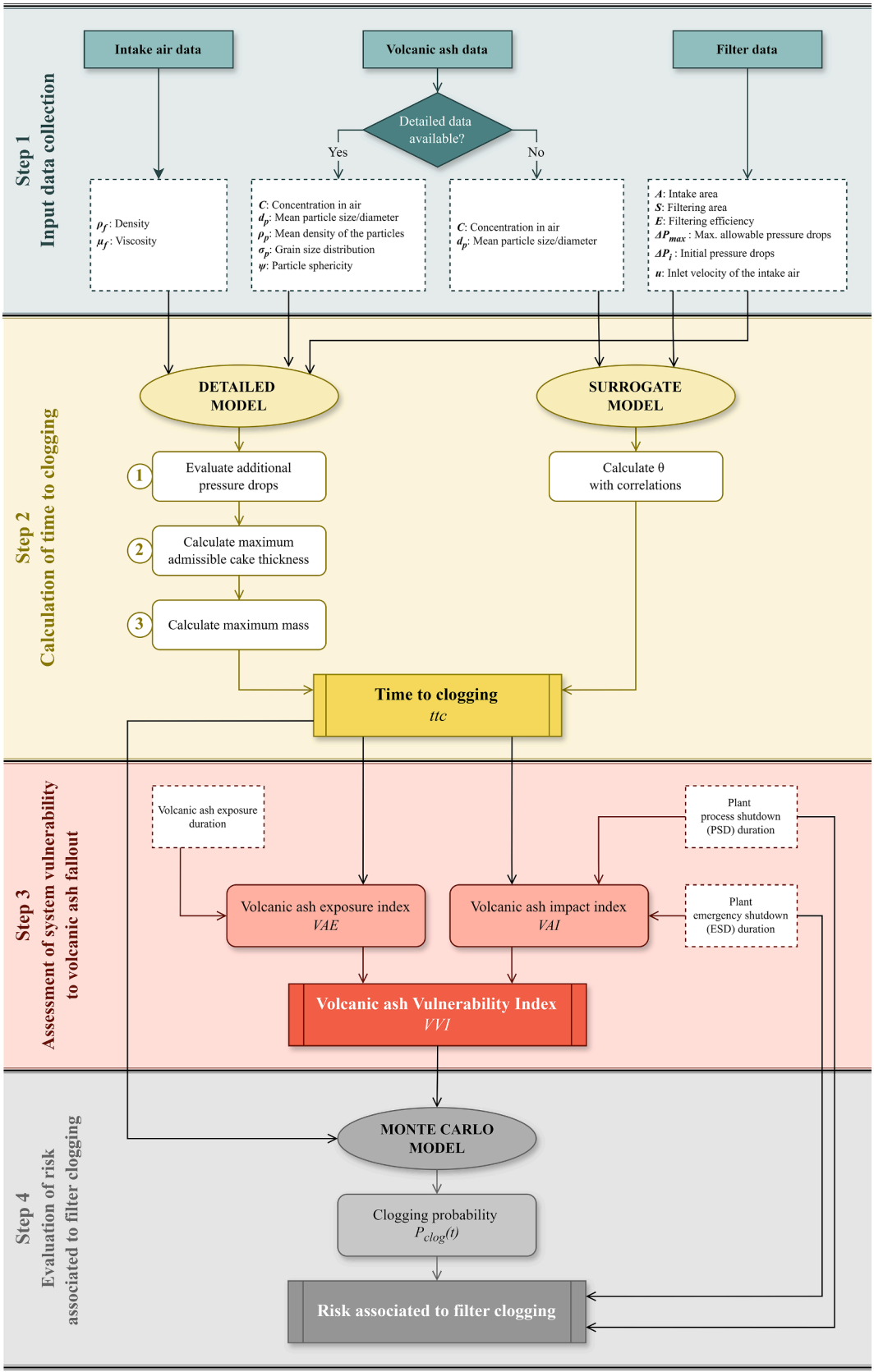

Fig. 2. Modelling approach and flowcharts of the models developed to assess the time to clogging of filtration systems and the vulnerability to potential cascading Natech events.

Table 1
Required input parameters for the detailed filter clogging model.

Category	Parameter	SI unit	Description
Intake air	ρ_f	kg/m^3	Density of the fluid
	μ_f	Pa•s	Viscosity of the fluid
Volcanic ash	C	g/ m^3	Concentration in air
	d_p	m	Mean particle size/diameter
	ρ_p	kg/m^3	Mean density of the particles
	σ_p	-	Grain size distribution
	ψ	-	Particle sphericity
Filter	A	m^2	Intake area
	S	m^2	Filtering area
	E	-	Filtering efficiency
	ΔP_{max}	Pa	Maximum allowable pressure drops
	ΔP_i	Pa	Initial pressure drops
	u	m/s	Inlet velocity of the intake air
Plant	t_{VAE}	s	Exposure time to volcanic ash
	t_{PSD}	s	Time for process shutdown completion
	t_{ESD}	s	Time for emergency shutdown completion

Table 2
Parameters used in Eq. (2) to evaluate the void fraction. Data from Hoffmann and Finkers [49].

Fitting parameter	Loosely packed	Tapped packed
α_1	0.416	0.320
α_2	−0.0142	−0.0371
α_3	−0.829	−1.72
α_4	0.862	0.848

pressure drops) changes if the cake formed is subject to compression. Specifically, a loosely packed cake is referred to bed in which items are arranged with extra space around them, allowing for movement and preventing a tight, structured fit. On the contrary, a tapped packing indicates a cake that undergoes compression (that may be induced, e.g., by system vibrations) until the items are tightly compacted, minimizing spaces and restricting movement.

2.3.2. Calculation of the maximum admissible cake thickness

Once the additional pressure drops per unit length in the cake are known, the maximum cake thickness before clogging can be evaluated. This value also depends on the maximum allowable pressure drop of the filter system before clogging, ΔP_{max} [Pa], and on the initial pressure drops, ΔP_i [Pa], during normal operation. Based on this information, the maximum cake thickness l_c [m] is calculated as reported in Eq. (3):

$$l_c = \frac{\Delta P_{\max} - \Delta P_i}{(-\Delta P/l)} \tag{3}$$

Noteworthy, the initial pressure drops, ΔP_i, shall take into account the pressure drops due to the filter cloth and the particulate matter deposited on the filter during normal operation.

2.3.3. Calculate maximum mass

The mass of volcanic ash that leads to the critical pressure drop, m_c [kg], is calculated using Eq. (4):

$$m_c = l_c \cdot S \cdot (1 - e) \cdot \rho_p \tag{4}$$

where l_c is the thickness of the volcanic ash cake that leads to the filter clogging as calculated in Eq. (3), S is the filter cross-sectional area [m^2], e is the void fraction of the cake [-], and ρ_p is the mean density of the particles [kg/m^3].

2.3.4. Time to clogging

The time to clogging ttc [s] is calculated based on the clogging mass, on the suction flow rate of the filtration system, and on the ash concentration in the air according to Eq. (5):

$$ttc = \frac{m_c}{u \cdot A \cdot E \cdot C} \tag{5}$$

where A is the intake area [m^2] (i.e., the internal area of the front filter frame), E is the filtering efficiency [-], and C is the concentration of the volcanic ash in the air [kg/m^3].

The calculation of the time to clogging using the procedure described above does not consider the time dependence of the ash characteristics. Among all, the concentration of volcanic ash may present a relevant dependence on time, especially when considering the early stages after the ashes reach the site of interest. When time variability of ashes concentration is relevant, a numerical integration may be used to calculate the time to clogging, as reported in Eq. (6):

$$ttc = \frac{m_c}{u \cdot A \cdot E \cdot \frac{1}{ttc - t_0} \cdot \int_{t_0}^{ttc} C(\tau) \cdot \mathrm{d}\tau} - t_0 \tag{6}$$

where t_0 is the initial time [s] considered in the evaluation. Noteworthy, two different values of the time to clogging can be obtained by applying the model: *i)* considering loosely packing, or *ii)* considering tapped packing condition. Since it is not possible to know a priori the condition of the cake formed, the two models may be considered the extreme conditions, and the actual ttc value will be in the range calculated using the apparent densities corresponding to the two alternative packing conditions.

2.3.5. Detailed model validation

Since specific experimental data concerning the time to clogging of filters are not available in the literature, model validation was based on experimental data addressing the relationship between filter mass loading and additional pressure drops caused by the bed of solid particles, that is the core element of the model. Two distinct experimental datasets were used for validation (Li et al. [50]; Wang et al. [51]). Table 3 summarizes the more important parameters used in the experimental runs. As evident from the table, the datasets concern different experimental conditions and filtration systems.

Fig. 3 reports a comparison between the additional pressure drops divided by gas velocity across the filter and the mass loading of the filter cake obtained in the experimental runs and by model simulation. Model results are shown for both the loosely packed and tapped packed conditions, which define the expected range of the actual pressure drops. As evident in the figure, most of the experimental data fall between the extreme model conditions. Experimental results outside the loosely/tapped range actually fall below the loose-cake prediction. Thus, the model provides conservative estimates of pressure drops for these conditions. Such outliers occur at low mass loadings, with maximum absolute errors lower than 80 Pa, which are consistent with experimental and modeling uncertainties. It should also be remarked that no experimental result exceeds the upper bound for pressure drops obtained assuming the tapped condition for the model.

2.4. Surrogate model

The application of the detailed model described above requires a

Table 3
Main parameters used in the experimental runs.

Parameters	Li et al. [50]	Wang et al. [51]
Filter type	Medium efficiency filter	High efficiency filter
Dust concentration [mg • m^{-3}]	70, 210	320, 1070, 1700, 3830, 7080
ISO 12103–1 test dust	A2 Fine test dust	A3 Medium test dust
Mean particle size [μm]	Distribution reported in the original study	6.54
Intake velocity [m • s^{-1}]	0.5, 1, 1.5, 2, 2.5, 3	0.1
Loading mass	20.1 - 378.2 g	37.6 - 2764.8 mg

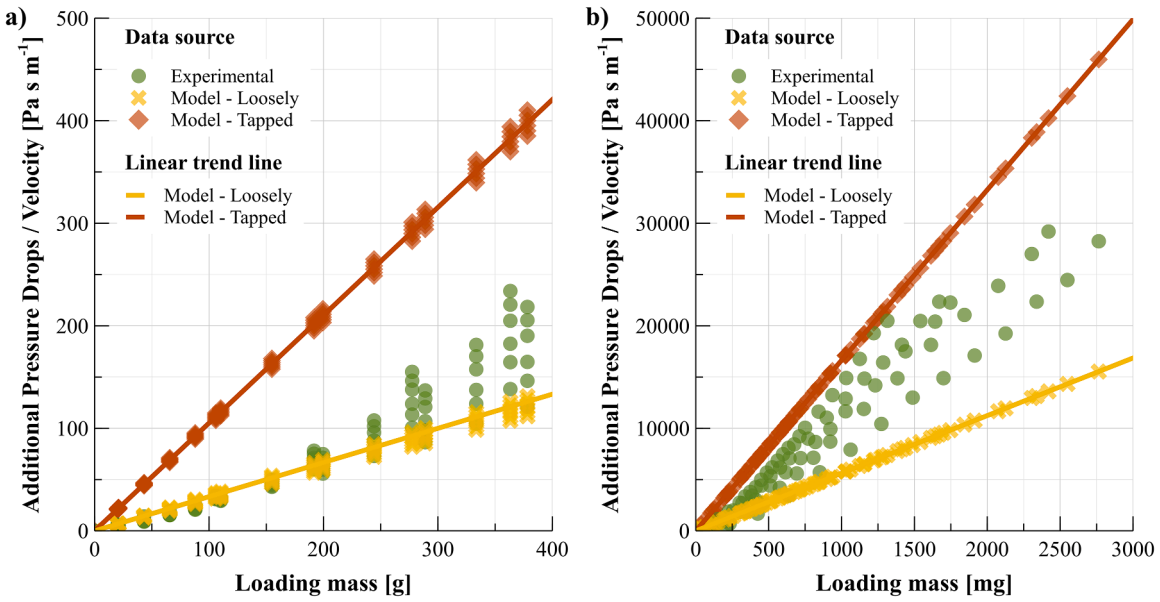

Fig. 3. Results of model validation: additional pressure drops divided by gas velocity versus the loading mass in the filter cake. Experimental data (green dots) are compared to model predictions for the tapped (red rhombuses) and loosely (yellow crosses) conditions. Linear trends obtained for model simulations are also reported. (a) Experimental data by Li et al. [50]; (b) Experimental data by Wang et al. [51].

significant effort for data collection, in particular with respect to the characteristics of the volcanic ashes, which may be difficult to obtain. Thus, a surrogate model was developed to calculate the time to clogging of filtration systems based on simplified correlations. This model enables an accurate and reliable estimation of the time to clogging using a reduced set of input parameters, thus allowing its application even in the absence of detailed data. To reach this goal, a specific procedure was followed to develop and validate the surrogate model, as described in Fig. 4.

2.4.1. *Identification of input parameters for the surrogate model*

The first step consisted of the identification of the input parameter for the surrogate model, aiming at the reduction of the number with respect to the detailed approach. The interdependences among the input parameters were first identified. As for the fluid, density and viscosity are required in the detailed model; at atmospheric pressure, both are critically dependent on fluid temperature T. Assuming a constant composition of the air, the temperature T can thus be considered as the single input parameter needed to characterize the fluid properties. Well-known correlations were used for the assessment of density and viscosity based on temperature [52].

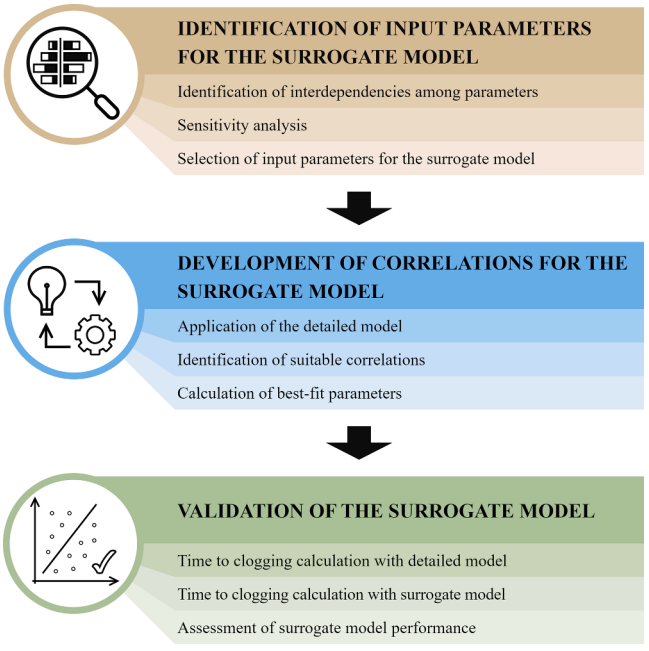

Fig. 4. Methodology for the development of the surrogate model for the calculation of the time to clogging of industrial filtration system exposed to volcanic ash fallout.

Regarding the volcanic ash properties, several previous studies have demonstrated that the density heavily relies on the particle size [53–55]. In the present study, the density correlation suggested by Pardini et al. [56] was considered for the development of the surrogate model. The expression is reported in Eq. (7), where d_p is the particle diameter [μm]:

$$\rho_p = \begin{cases} 2500 & d_p < 7.81\mu\text{m} \\ 2500 - \dfrac{d_p - 7.81}{1000 - 7.81} \cdot (2500 - 1000) & d_p \in [7.81, 1000]\mu\text{m} \\ 1000 & d_p > 1000\mu\text{m} \end{cases} \tag{7}$$

A sensitivity analysis was then carried out to assess the impact of the uncertainty related to input parameters on the results. The input parameters considered are those related to the volcanic ash, fluid temperature, and air intake velocity. Although the latter typically remains at a nominal value, the intake velocity can vary depending on operational needs and significantly impacts the *ttc* value, as shown in Eq. (5). On the contrary, the other features of the filter were excluded from the sensitivity analysis, since they are well-defined once the system is known.

The analysis was carried out applying a Global Sensitivity Analysis (GSA) approach, as it enables to include also the interactions among input parameters. Indeed, the use of GSA addresses the challenge of determining a nominal value for the parameters, which is not straightforward in the case of volcanic ash characterization. Table 4 shows the credible variability range selected for each parameter based on literature data.

The GSA was performed using the Morris method [59–61], considering 6 samples equally distributed for each parameter reported in Table 4. More information on the method is reported in the available

Table 4
Input parameters considered in the GSA and their assumed variability range.

Parameter	Variability range Min	Max	Reference
d_p [μm]	50	1000	[56]
σ_p [-]	0	0.69	[49]
ψ [-]	0.5	0.8	[57]
C [μg/m^3]	200	4000	[58]
T [°C]	−30	60	To cover almost all environmental conditions
u [m/s]	1.78	4.46	Based on commercially available filtration systems

literature [59–61]. Two sensitivity indices were calculated for each parameter: the absolute mean, AM_{GSA}, and the standard deviation, SD_{GSA}. The absolute mean indicates the magnitude through which a parameter affects the model output. A high value of AM_{GSA} indicates that the input variable has a strong influence on the model output. The standard deviation, instead, measures the variability in the influence that arises from interactions with other parameters. A high value of SD_{GSA} indicates that the effect of the parameter on the model output strongly depends on the values of other inputs, highlighting interactions among input parameters.

To perform the GSA, two filters with significantly different characteristics (summarized in Table 5) were selected to ensure that system properties do not influence the results. Eventually, the analysis was performed using both loosely and tapped packing parameters for void fractions.

The results of the sensitivity analysis are presented in Fig. 5. A qualitatively similar behavior can be observed considering the two filter systems, confirming a moderate influence on the ranking of parameters. The concentration of volcanic ash (C) shows the highest values of both AM_{GSA} and SD_{GSA}. This indicates that C strongly affects the time to clogging, and that the effect is also influenced by the value of the other parameters. Similar conclusions can also be drawn considering intake velocity (u) and the mean particle size (d_p). On the contrary, modest values of the absolute mean and of the standard deviation are obtained by the sphericity of the particles (ψ), the grain size distribution (σ_p), and the temperature (T), implying that their effects on clogging time are respectively less influent and less dependent on the other parameters. Thus, these parameters are excluded from the input of the surrogate model. This choice is also supported by the high variability and uncertainty related to these characteristics of volcanic ashes. Finally, the loose packing condition is associated with higher AM_{GSA} and SD_{GSA} than the tapped packing case, indicating higher model sensitivity to the input parameters in this regime.

Based on the results of the sensitivity analysis, the input parameters selected for the surrogate model are the intake velocity (u) of the filter, the particle concentration in air (C), and the mean particle size (d_p) of the ashes.

In the development of the surrogate model, a narrow size distribution of volcanic ash particles is assumed, considering σ_p equal to 0.0375 as suggested by Hoffmann and Finkers [49]. This assumption is supported by the significant decrease in the grain size distribution observed at increasing distances from the eruption site [56,64]. As for sphericity (ψ), a conservative approach was adopted, selecting the upper bound of the variability range (i.e., 0.8) since it yields the lower values of the time to clogging. Similarly, to obtain conservative results, a temperature equal to −30 °C is selected for the development of the surrogate model.

Table 5
Characteristics of the filters used in the GSA.

Filter:	Filter A	Filter B
Class to EN779:2012	G4	M6
A [m^2]	0.311	0.350
S [m^2]	1.8	9
E_{PM10} [%]	51	77
$E_{PM>50}$ [%]	100	100
ΔP_{max} [Pa]	375	450
ΔP_i [Pa]	$\Delta P_i = 4.771\ u^2 - 2.527\ u + 5.95$	$\Delta P_i = 3.344\ u^2 + 4.014\ u + 15.63$
Reference	[62]	[63]

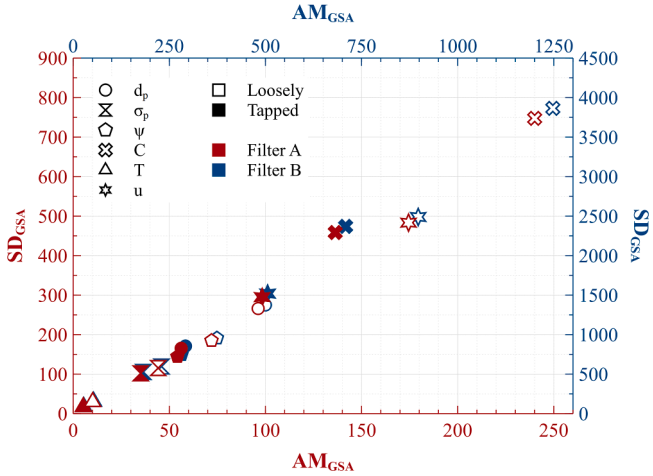

Fig. 5. Results of the GSA for the parameters defined in Table 4 and the filters types described in Table 5 considering both the loosely and tapped packing parameters for the assessment of the void fraction of the cake.

2.4.2. Development of surrogate model correlations

The second step of the surrogate model development focuses on the correlations to calculate the time to clogging. Dependences of filtration system parameters and concentrations were thus isolated from the model equations. Consequently, the time to clogging can be expressed as reported in Eq. (8), where θ is defined by Eq. (9):

$$ttc = \theta \cdot \frac{S \cdot (\Delta P_{max} - \Delta P_i)}{A \cdot E \cdot \frac{1}{ttc - t_0} \cdot \int_{t_0}^{ttc} C(\tau) \cdot d\tau} - t_0 \tag{8}$$

$$\theta(d_p, u) = \frac{(1-e) \cdot \rho_p}{(-\Delta P/l) \cdot u} \tag{9}$$

The dependence of θ from d_p is implicit in the value of e, ρ_p, and $-\Delta P/l$ as indicated in Eqs. (2), 7, and 1 respectively. It is worth mentioning that when the concentration of volcanic ashes is constant with time, a simplified version of Eq. (8) can be obtained in analogy with those presented for the detailed model (see Eq. (5)).

The detailed model was applied to calculate θ in a wide range of conditions. Specifically, the input parameters of the surrogate model (i.e., d_p and u) were uniformly sampled within the variability range defined in Table 4. 21 samples for each input parameter were considered and combined together to generate a set of input vectors (i.e., 441 combinations). The combinations were then used to calculate two different datasets for θ, each considering respectively the formation of a loosely or a tapped packing cake of volcanic ash on the filtration panel. As a result, two sets of empirical correlations were developed to assess the time to clogging.

The value of θ as a function of the intake velocity is reported in Fig. 6 for different mean particle diameters, considering both the loosely (white-filled) and tapped (black-filled) packing of the cake. As can be observed, a power law dependence may be used to relate θ to u:

$$\theta = A \cdot u^B \tag{10}$$

The values of the A and B coefficients in the correlation reported in Eq. (10) were calculated considering each particle diameter and packing

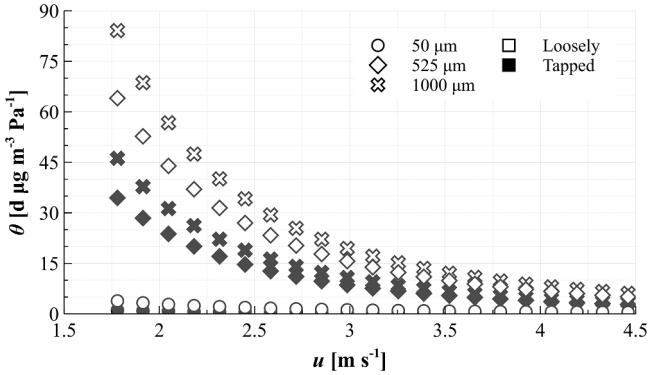

Fig. 6. Trend of θ as a function of the intake velocity u considering different values of mean particle size d_p and the two extreme packing conditions (loosely and tapped) of the volcanic ash filter cake.

condition. The dependence of these parameters was then investigated as a function of d_p, and the results are reported in Fig. 7.

Specific correlations for A and B as a function of the particle diameter were then developed. Regarding parameter A, Fig. 7-a shows a polynomial trend with particle diameter for both packing conditions. Specifically, a fourth-degree polynomial was chosen for the correlation, as reported in Eq. (11), providing a reasonable trade-off between the accuracy of the fit and the number of parameters:

$$A = a_1 \cdot {d_p}^4 + a_2 \cdot {d_p}^3 + a_3 \cdot {d_p}^2 + a_4 \cdot d_p + a_5 \tag{11}$$

As for parameter B, a power law provided the best correlation between the data and the particle diameter, as reported in Eq. (12). In this case as well, two distinct sets of parameters were evaluated based on the packing conditions of the cake. Although the values appear very similar in Fig. 7-b considering loosely and tapped conditions, parameter B represents the exponent in Eq. (10), thus exerting a significant influence on the final θ value even in front of limited variations of B.

$$B = b_1 \cdot {d_p}^{b_2} \tag{12}$$

Table 6 provides the fitting coefficients to be used in Eqs. (11) and (12) to calculate the final θ value according to Eq. (10).

2.4.3. Validation of the surrogate model

Fig. 8 compares the results obtained by the detailed (data points) and surrogate (dotted lines) models. Specifically, Fig. 8 reports the θ value as a function of the intake velocity for different particle diameters considering both the loosely (panel a) and tapped (panel b) packing conditions for the volcanic ash cake. As can be seen from the examples reported in the figure, the surrogate model provides a good approximation of the detailed results.

A validation dataset of 2500 entries was considered for the input parameters in order to compare the results of the detailed and surrogate models. The dataset was built from the combination of 50 equally distributed values of d_p and u in the variability range defined in Table 4.

Table 6
Values of the best-fit coefficients to be used in Eqs. (11) and (12) considering the loosely and the tapped correlation for the cake void fraction.

Fitting parameter	Loosely	Tapped
a_1	8.396E-10	3.956E-10
a_2	−2.410E-06	−1.184E-06
a_3	1.827E-03	9.206E-04
a_4	0.1798	0.1076
a_5	−1.469	−4.618
b_1	−1.655	−1.585
b_2	0.07932	0.08437

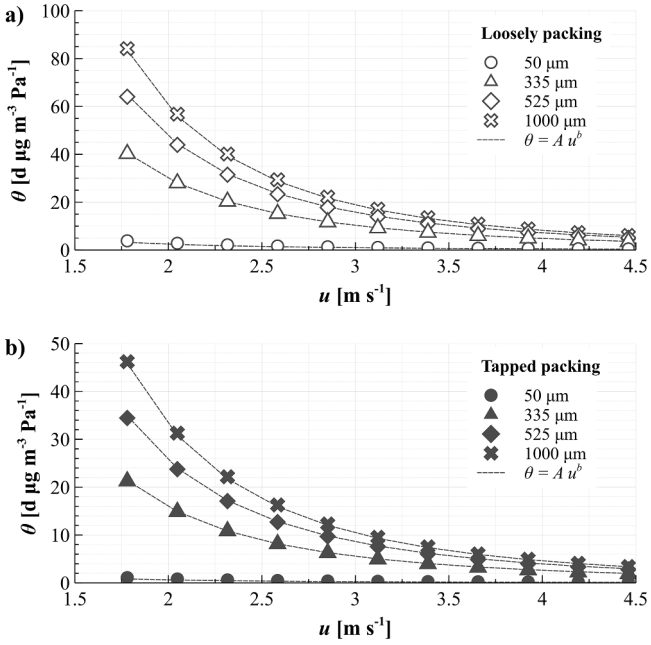

Fig. 8. Comparison of the results of the detailed (data points) and surrogate (dotted lines) models for both loosely packed (a) and tapped packed (b) filter cakes.

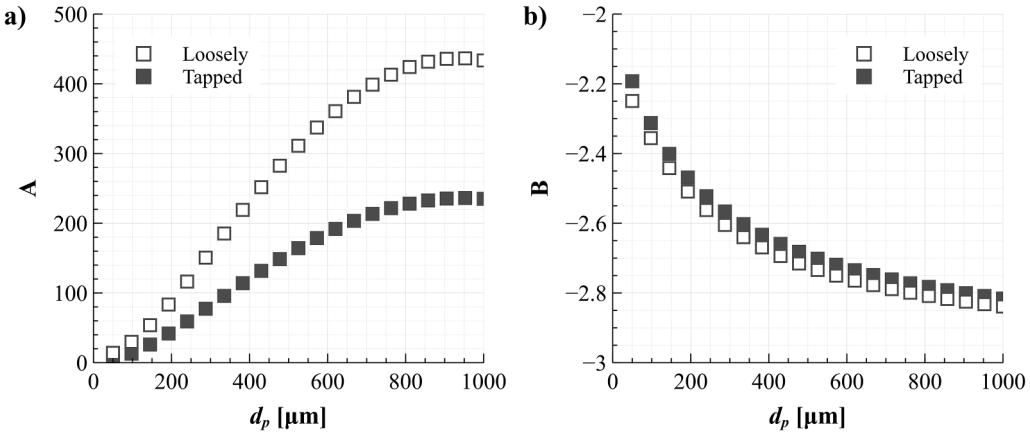

Fig. 7. Trends of the correlation parameters A (a) and B (b) with respect to the mean particle size d_p considering loosely and tapped conditions for the packing of the volcanic ash filter cake.

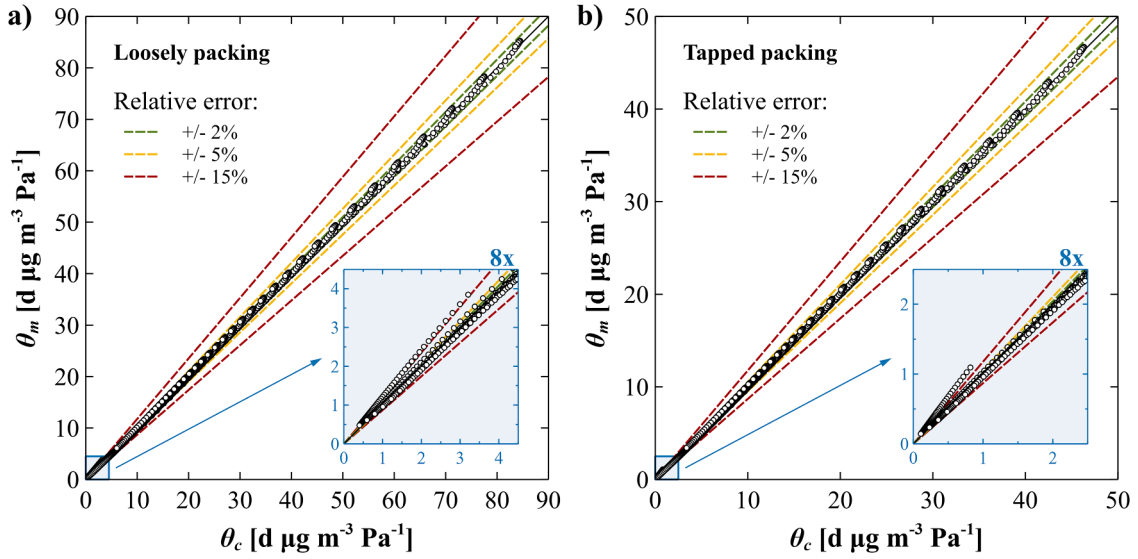

Fig. 9. Parity plots comparing the θ values obtained from the detailed and the surrogate model obtained considering (a) loosely packing conditions and (b) tapped packing conditions.

Fig. 9 shows the parity plot reporting the values of θ calculated using the two models.

As shown in Fig. 9, the surrogate model has a satisfactory performance both in the case of the loosely (panel a) and tapped (panel b) packing conditions. The figure also reports three thresholds for the relative error (2 %, 5 %, and 15 %). The error is scarcely affected by the type of packing considered for ash cake. As shown in the figure, more than 60 % of the data points have errors lower than 2 % (green lines in Fig. 9), and more than 95 % of the data points have relative errors lower than 5 % (yellow lines). A total of 98 % of the data points show relative errors lower than 15 % (red lines). However, relative errors exceeding 15 % are present only when considering very low particle diameters and high velocities. These conditions lead to very low values of θ, lower than approximately 4 d•µg•m^{-3}•Pa^{-1} under loosely packed conditions and lower than 2 d•µg•m^{-3}•Pa^{-1} under tapped packing conditions (bottom right squares in Fig. 9). Low times to clogging are obtained in this condition, thus the absolute error in the assessment of such parameter is limited. It should also be remarked that the surrogate model provides a conservative estimate of the time to clogging, as it predicts lower values of θ (and therefore of *ttc*) than the detailed model.

Additional indicators used to evaluate the correlation performance of the surrogate model are reported in the Supplementary Material.

2.5. Step 3: assessment of system vulnerability to volcanic ash fallout

The time to clogging of filtration systems represents a relevant parameter to assess the vulnerability to volcanic ash of critical utilities and services, such as process air or instrument air. The model derived for the time to clogging was thus coupled to a risk matrix enabling the screening of the potential hazard [65,66]. The use of risk matrices is broadly recognized in engineering standards (e.g., ISO 17776 [67]) and in the scientific literature [68,69] as a useful, practical, simple, transparent, and conservative tool to support risk-based decisions. Clearly enough, the qualitative risk screening obtained from the matrix approach allows the identification of critical equipment requiring a detailed risk assessment to prevent discontinuity in operation and/or Natech scenarios, addressing both the expected exposure to ash fallout phenomena and the consequences of end-point scenarios deriving from filter clogging.

The matrix proposed in this study was thus specifically developed to support risk screening for volcanic ash-induced filter clogging. The matrix is based on the assessment of volcanic ash exposure (*VAE*) and volcanic ash impact (*VAI*) indexes. The *VAE* index is defined considering three different scenarios, based on the comparison of the *ttc* with the period for which relevant concentrations of volcanic ashes are present at the industrial site of interest, t_{VAE}, as shown in Table 7.

The *VAI* index, addressing the assessment of the potential impact of the volcanic ash, was defined considering four scenarios, based on the comparison of the *ttc* with two reference values for the completion of site shutdown procedures: the time required for process shutdown, t_{PSD}, and the time required for emergency shutdown, t_{ESD}. The values assumed for the *VAI* index are summarized in Table 8 together with a description of the expected impact.

It should be highlighted that the time required to complete the process and emergency shutdown procedures, used to define the *VAI*, depend on the complexity of the plant and are strongly process- and plant-specific. Actually, shutdown completion may require times ranging from a few hours to several days, as evidenced by Misuri et al. [70]. However, such data are usually well-known by the plant manager and operators.

Fig. 10 shows the vulnerability matrix defined to assess vulnerability to volcanic ash based on the exposure (*VAE*) and impact (*VAI*) indexes.

As shown in the figure, five vulnerability categories are defined, depending on the clogging probability and on the possible consequences, ranging from very low to very high. A very low vulnerability is obtained when no clogging occurs or the *ttc* is higher than the time required to complete process shutdown procedures. In such cases, continuous monitoring of both the evolution of the volcanic event and filter pressure drop can be sufficient, possibly not requiring the actual implementation of process shutdown. On the contrary, a very high vulnerability is present when the filter clogging probability is high and the time to clogging is lower than the time required for the emergency shutdown. In these conditions, business interruption is required and

Table 7
Definition of the volcanic ash exposure *VAE* index.

Volcanic ash exposure *VAE*	Range	Meaning
LOW (1)	$t_{VAE} < ttc_T$	Low credibility of clogging occurrence
MEDIUM (2)	$ttc_T < t_{VAE} < ttc_L$	Moderate credibility of clogging occurrence
HIGH (3)	$t_{VAE} > ttc_L$	High credibility of clogging occurrence

Table 8
Definition of the volcanic ash impact *VAI* index.

Volcanic ash impact *VAI*	Range	Meaning
LOW (1)	$t_{PSD} < ttc_T$	• Compatible with the activation and safe completion of process shutdown procedures • Clogging before process shutdown not credible • Business interruption unless backup available
MEDIUM (2)	$t_{ESD} < ttc_T < t_{PSD}$	• Compatible with the activation and safe completion of emergency shutdown procedures • Clogging before emergency shutdown not credible • Possible issues due to emergency shutdown activation • Business interruption unless backup available
HIGH (3)	$ttc_T < t_{ESD} < ttc_L$	• Activation of emergency shutdown procedures • Possible clogging during emergency shutdown procedures • Possible lack of utility systems due to filter clogging • Possible issues due to emergency shutdown activation • Business interruption possible even in the presence of backup
VERY HIGH (4)	$ttc_L < t_{ESD}$	• Activation of emergency shutdown procedures • Clogging likely during emergency shutdown procedures • Credible lack of utility systems due to filter clogging • Issues in emergency shutdown completion due to lack of utility systems • Business interruption likely even in the presence of backup • Possible development of indirect Natech scenarios

possible secondary Natech accidents may occur due to the unavailability of instrument air, causing the unavailability of critical utility systems.

2.6. Step 4: evaluation of risk associated to filter clogging

For the vulnerable sites and systems identified by the matrix screening approach described in Section 2.5, the risk associated to filter clogging may be quantified considering the safety implications for plant operation. In particular, these may be derived by the comparison of the time to clogging to the characteristic times of the shutdown procedures, process and emergency shutdown. Clearly enough, if clogging occurs at times lower than the emergency or process shutdown, unsafe operation scenarios may take place, leading to near miss or accident scenarios. In particular, three different regions may be identified: *i)* an accident/near miss region, where time to clogging is lower than the time to emergency shutdown; *ii)* an unsafe process shutdown region, where the time to clogging is higher than the time to emergency shutdown but lower than the time to process shutdown; and *iii)* a safe region, where the time to clogging is higher than both the time to emergency shutdown and the time to process shutdown. A quantitative model for filter clogging has thus been developed in order to assess the probability of accident/near miss or unsafe shutdown for a specific filter and exposure scenario.

A Monte Carlo (MC) model has thus been developed to assess the filter-specific probabilistic clogging probability with respect to time. The flowchart of the procedure is reported in Fig. 11. In the MC model, the initial pressure drop ΔP_i is assumed as a random variable, sampled from a distribution spanning from the value corresponding to a new filter to the typical replacement threshold adopted at the plant. For each iteration, a random $\Delta P_i(iter)$ is generated, and the corresponding times to clogging $ttc_T(iter)$ and $ttc_L(iter)$ are computed. The clogging probability at a given time since the start of the exposure scenario, $P_{clog}(t, iter)$, for the specific iteration *iter* and time *t* is then evaluated through Eq. (13):

$$P_{clog}(t, iter) = \begin{cases} 0 & t \le ttc_T(iter) \\ \dfrac{t - ttc_T(iter)}{ttc_L(iter) - ttc_T(iter)} & ttc_T(iter) < t < ttc_L(iter) \\ 1 & t \ge ttc_L(iter) \end{cases} \quad (13)$$

The times to clogging under tapped and loosely packed conditions (ttc_T and ttc_L) are considered as the two limiting bounds of the system response, and a uniform distribution of the actual clogging time between these two limiting values is assumed. A uniform distribution is also assumed for the pressure drop of the filter system $\Delta P_i(iter)$ at the onset of the exposure scenario, reflecting the hours of operation of the filter since the last replacement.

After all iterations are performed for a given time, the overall probability of clogging $\overline{P}_{clog}(t)$ is obtained as the average value across all iterations, as reported in Eq. (14).

$$\overline{P}_{clog}(t) = \frac{\sum_{iter=1}^{N_{iter}} P_{clog}(t, iter)}{N_{iter}} \quad (14)$$

The MC model can be integrated either with the detailed or the surrogate model for the calculation of the time to clogging. The choice of the model for the *ttc* calculation does not affect the MC procedure reported in Fig. 11, only affecting the input parameters required for the definition of the volcanic ash scenario, which must be selected consistently with the model selected for time to clogging calculation (see Fig. 2). Clearly enough, both constant and time-dependent concentrations of volcanic ash particles can be considered in the MC model for the quantification of risks due to filter clogging developed in the present study.

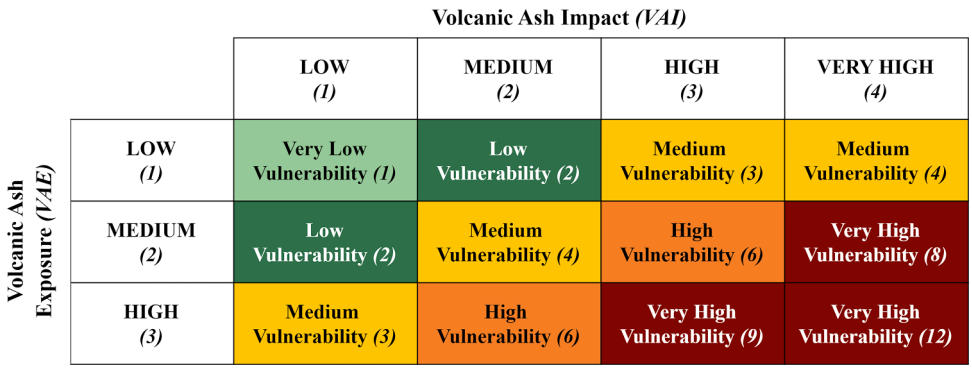

Fig. 10. Vulnerability matrix defined for system failures due to the possible unavailability of process and/or instrument air caused by volcanic ashes. *VAE* and *VAI* indexes are defined in Table 7 and Table 8 respectively.

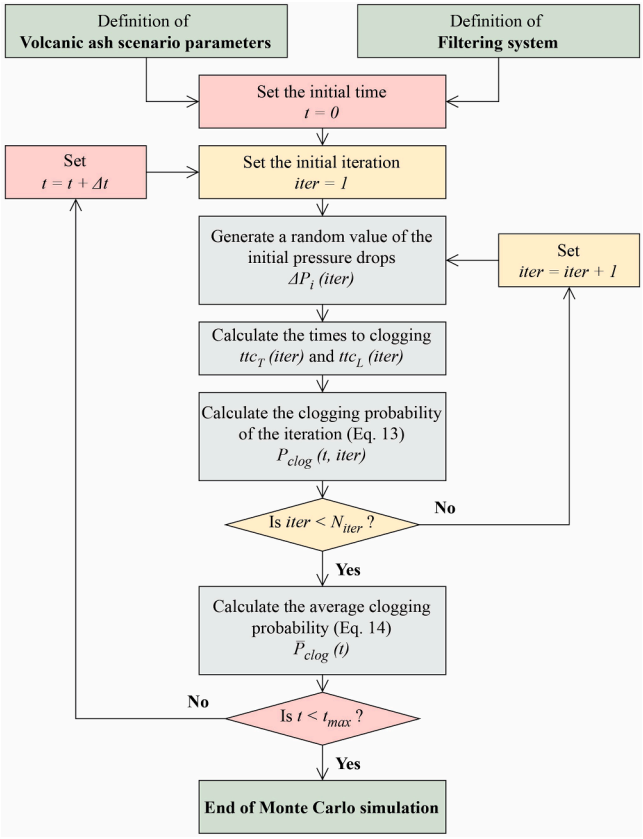

Fig. 11. Flowchart of the Monte Carlo procedure for the calculation of the clogging probability as a function of time.

3. Test cases

Two test cases addressing significant examples of applications of the methodology have been defined to demonstrate its applicability and to test model performance under different scenarios. Test bed 1 aims at investigating the effects on the time to clogging of the particle size, of the ash concentration in air, and of the filtration system characteristics. Test bed 2 investigates the effects of the distances from the eruption site based on realistic literature data for the concentration and diameter of the ashes. Test bed 2 is also used to show the results of the calculation of the clogging probability using the MC model developed.

3.1. Test bed 1

Three particle diameters (100 μm, 300 μm, and 800 μm) and three concentrations of volcanic ashes dispersed in the air (1000 μg/m^3, 2500 μg/m^3, and 4000 μg/m^3) have been considered for the calculation of the time to clogging. Eight filtration systems are taken into account, and their features are described in Table 9. The data included in the table concern commercial industrial filtration systems [71] belonging to several categories defined by the EN 779:2012 standard [72]. In addition, a parametric analysis is carried out to investigate the influence of the concentration and particle diameter on the time to clogging for three specific filtration systems, selected to represent the three filter classes defined by EN 779:2012: Filter 3 (coarse), Filter 5 (medium), and Filter 8 (fine).

3.2. Test bed 2

Six exposure scenarios based on realistic data are defined. Table 10 reports the features of the selected scenarios. As evident from the table, scenarios from 1 to 4 were obtained considering an average diameter for the particles in the range of those evaluated by Pardini et al. [56] in the analysis of the volcanic ash atmospheric dispersal process of eruptive scenarios. Fig. 12-a shows the concentration curves assumed in the analysis of the scenarios. These were adapted from those reported by Devenish et al. [73] related to the eruption of the Eyjafjallajökull volcano in April 2010, assuming a log-normal distribution of the concentration over time. The time durations of the exposure to the ash cloud were derived from the data reported by Biass et al. [74].

Two further scenarios (5 and 6 in Table 10) were considered to assess the potential long-range impacts of volcanic ashes, using concentration data derived from the London Volcanic Ash Advisory Center (VAAC) [78] for the eruption of the Krafla volcano (Island) occurred on January 12th, 2024. Fig. 13 shows the positions of the two industrial sites considered in Scenarios 5 and 6. The concentrations considered in the analysis of the scenarios are shown in Fig. 12-b.

In all scenarios, the surrogate model was applied for the calculation of the time to clogging, accounting for the time dependence of the concentration.

For the calculation of the clogging probability by the MC model (Step 4 in Fig. 2), the initial pressure drops ΔP_i are considered to range between the value reported in Table 9 and the replacement value (set equal to 90 % of the maximum allowable pressure drops in Table 9). A number of iterations equal to 10^6, a maximum time of exposure equal to 10 d, and a time step equal to 0.1 h are considered in the MC model.

4. Results

Fig. 14 shows the results obtained using the surrogate model for the time to clogging of the filtration systems included in the first test bed. Panels (a) and (b) show the dependence of *ttc* on the concentration and on the specific filtration system considering a particle diameter of 300 μm. Panels (c) and (d) show the time to clogging calculated considering a fixed concentration of 2500 μg/m^3. The qualitative trend obtained is similar for all the other particle diameters and concentrations considered in the test bed. For the sake of brevity, the complete results obtained for test bed 1 are thus reported in Tables S2 and S3 of the supplementary material, which also includes a thorough comparison of the performance of the surrogate model with respect to the detailed model developed in the present study.

As shown in Fig. 14 and in the Supplementary Material, the values obtained for *ttc* range from about six hours to several tens of days. The high variability of the *ttc* is in line with the large variations in the input

Table 9
Main parameters of the filtration systems considered in test bed 1. Data from [71].

Filter parameter	Filter 1	Filter 2	Filter 3	Filter 4	Filter 5	Filter 6	Filter 7	Filter 8
EN779:2012 class	G3	G4	G4	M5	M6	M6	F7	F8
A [m^2]	0.3505	0.3114	0.3505	0.3505	0.3505	0.3505	0.3505	0.3505
S [m^2]	4	1.8	6	4	6	9	9	9
E_{PM10} [%]	44	51	48	58	61	77	86	95
$E_{PM>50}$ [%]	82	100	100	100	100	100	100	100
ΔP_{max} [Pa]	250	375	250	450	450	450	450	450
ΔP_i [Pa]	20	62	50	50	65	80	100	140
Nominal u [m•s^{-1}]	2.5	3.8	2.7	3.2	3.2	3.2	3.2	3.2

Table 10
Input data used for test bed 2.

Features	Scenario 1	Scenario 2	Scenario 3	Scenario 4	Scenario 5	Scenario 6
Distance from the eruption site [km]	10	20	30	40	1150	1600
Particle diameter d_p [μm]	795	379	186	131	50[a]	50[a]
Filter system (see Table 9)	Filter 2	Filter 2	Filter 2	Filter 2	Filter 2	Filter 4
Time for process shutdown completion[b] t_{PSD} [h]	36	60	96	108	48	120
Time for emergency shutdown completion[b] t_{ESD} [h]	12	24	48	36	12	60

[a] Particle diameter assumed as suggested by [56,75-77] considering a relevant distance from the eruption site.
[b] Adapted from Misuri et al. [70].

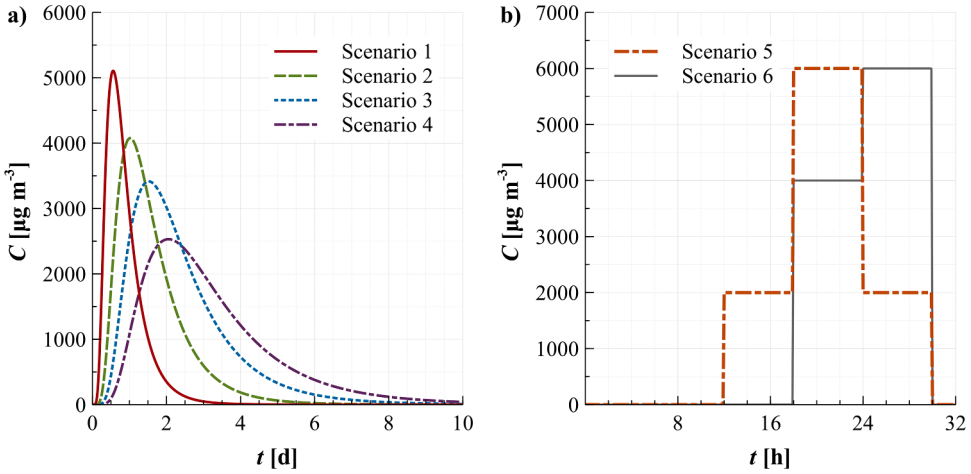

Fig. 12. Volcanic ash concentration vs. time assumed for (a) Scenarios 1 to 4, derived from the data reported by Devenish et al. [73]), and (b) Scenarios 5 and 6 (based on data from the London VAAC [78]).

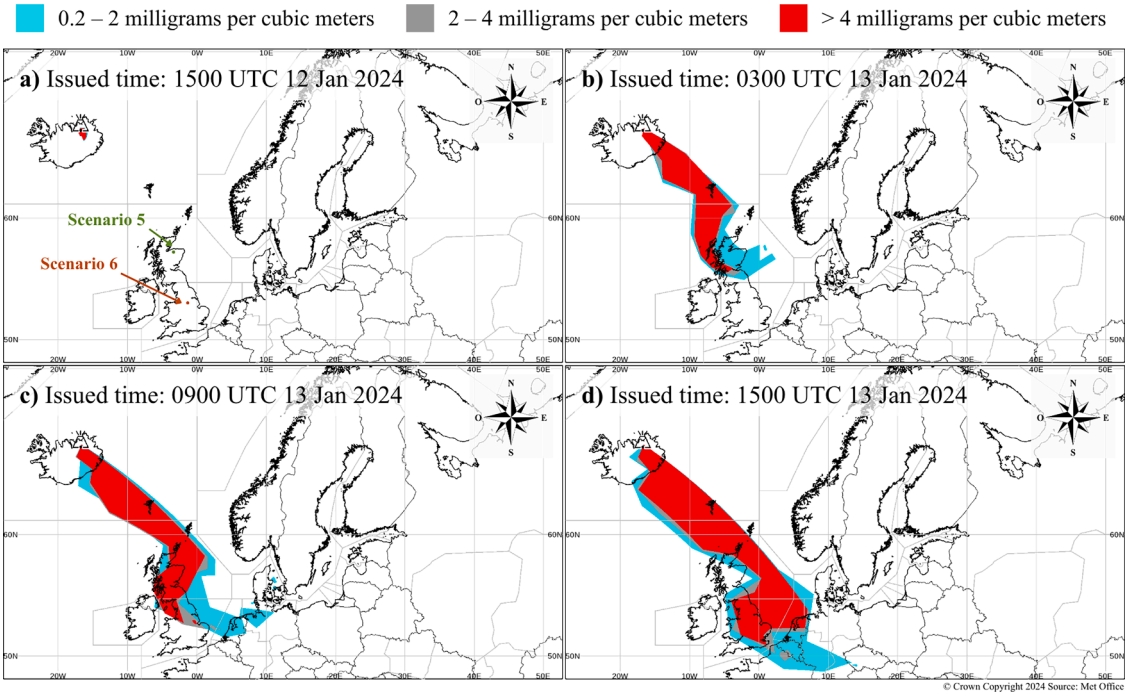

Fig. 13. Maps of the concentration of volcanic ash as a function of the time assumed in Scenarios 5 and 6 in Table 10. Data adapted from the London VAAC [78].

parameters considered in the Test Bed (see Section 3.1).

Fig. 14 allows evaluating the influence of the filtration system on the *ttc*. Filtration systems classified as G according to the EN779:2012 standard (filters F1-F3) are the most vulnerable to volcanic scenarios, exhibiting lower values of the time to clogging compared to higher class filters (class M: filters F4-F6, class F: filters F7-F8). This is due to the limited allowable differences between maximum and initial pressure drops, and to the lower ratio between the filtration area and the intake area compared with other filter classes. As shown in Eq. (8), these two parameters are critical in calculating the time to clogging. Among all

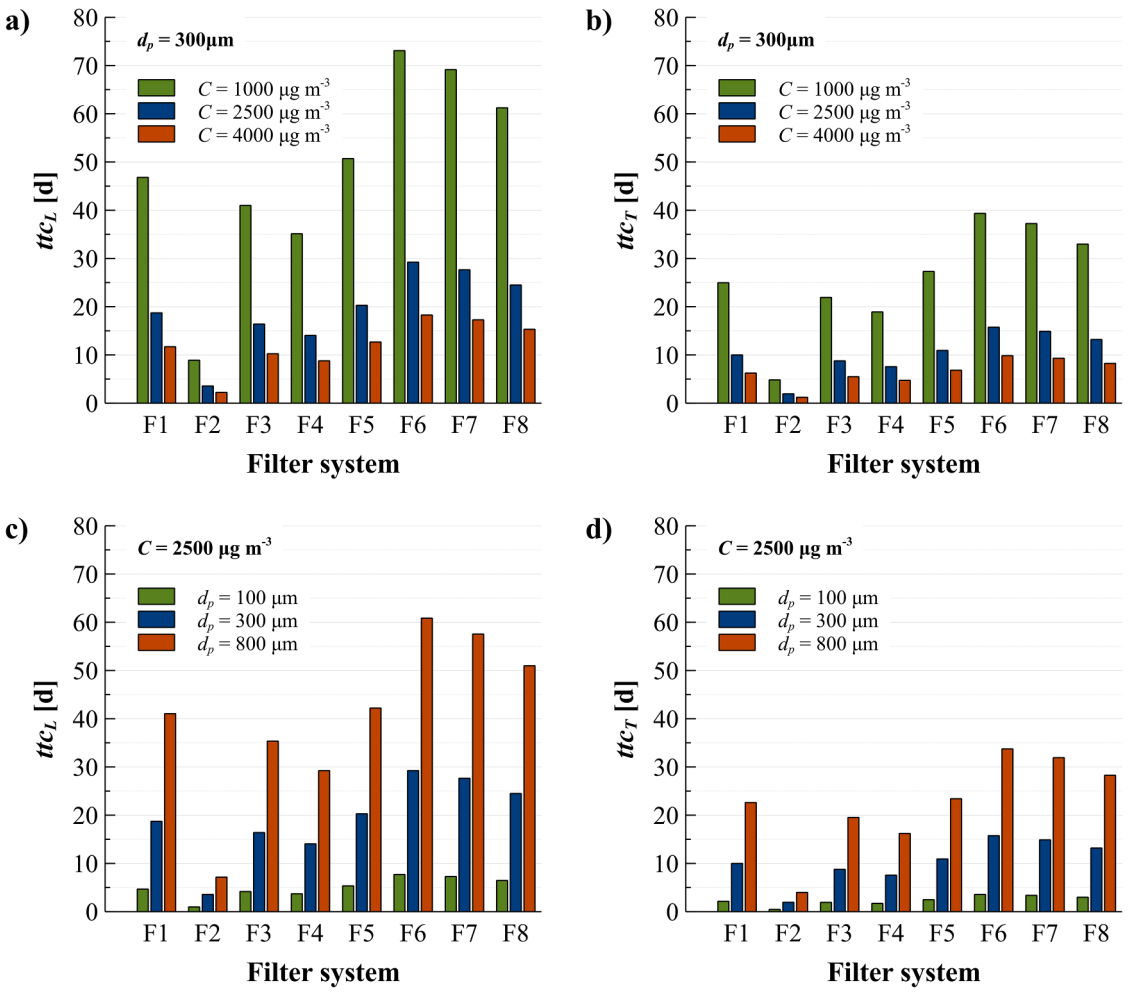

Fig. 14. Results of test cases included in Test Bed 1. Time to clogging calculated for the filtration systems listed in Table 9 considering: (a) three different concentrations, a particle diameter of 300 µm and the loosely correlation; (b) three different concentrations, a particle diameter of 300 µm and the tapped correlation; (c) three different diameters, a concentration of 2500 µg•m^{-3} and the loosely correlation; and (d) three different diameters, a concentration of 2500 µg•m^{-3} and the tapped correlation.

filter systems, F2 is particularly vulnerable (see Table 9) as it exhibits the lowest filtering area to intake area (*S/A*) ratio, modest allowable pressure drops, and a high nominal intake velocity compared to other filters belonging to the same class.

Fig. 15 shows the results of a parametric analysis, providing a detailed insight into the variation of the time to clogging as a function of the ash particle concentration and particle diameter. In panels (a) and (b), the time to clogging is evaluated as a function of the concentration of particles in the air. The time to clogging exhibits a sharp decline with the increase of the concentration across all filter types and particle diameters. As expected, high-performance filters (e.g., Filter 8) show higher *ttc* both considering loosely (Fig. 15-a) and tapped (Fig. 15-b) packings.

As shown in Fig. 15-c and d, the higher void fractions of cakes formed by larger particles result in an increasing time to clogging with particle size, reaching a maximum at diameters of approximately 850 µm. Above this value, the obstruction of the cross-sectional flow area caused by the particles prevails, causing a slight decrease in the time to clogging for increasing particle sizes. Overall, as expected, the more critical scenarios for filtration systems are caused by ash clouds with a high concentration and small particle diameters.

Fig. 16 shows the results obtained from Scenarios 1 to 4 in Test Bed 2. The figure reports both the time to clogging and the concentration vs. time curve assumed for each scenario. It should be remarked that the same filtering system is considered in all the scenarios to allow a significant comparison of the results (see Table 10).

As shown in the figure, in Scenario 1 the filter clogging does not occur due to the low concentrations and limited duration of the exposure (see Fig. 16-a). In Scenario 2 (Fig. 16-b), clogging occurs after 3.9 days when considering a tapped packing, while no clogging occurs if loose packing is considered. Since ttc_T and ttc_L represent extremes in the evaluation, this situation highlights a non-negligible vulnerability of the system to the volcanic ash scenario considered. Conversely, the time to clogging is shorter than the duration of the exposure regardless of the packing conditions for Scenarios 3 and 4 (panels c and d in Fig. 16, respectively). This indicates that the shutdown of the filtration system is required due to the ash load, leading to possible cascading events.

Similar results are obtained when analyzing the last two scenarios included in the second test bed, reported in Figure S2 of the Supplementary Materials. Scenario 5 presents a *ttc* value lower than the exposure time considering both loosely (ttc_L = 20.2 h) and tapped (ttc_T = 15.3 h) correlations. In Scenario 6, clogging occurs after about 1 day when considering a tapped packing, while no clogging occurs if a loose packing is considered, as in the case of Scenario 2.

Fig. 17 shows the results of the vulnerability assessment of the air intake systems for the 6 scenarios considered in Test Bed 2. As shown in the figure, depending on the scenario and the time required for system shutdown, very different vulnerability rankings are obtained. It is worth remarking that, depending on the scenario, high values for both the Volcanic Ash Exposure *VAE* and the Volcanic Ash Impact *VAI* indexes are

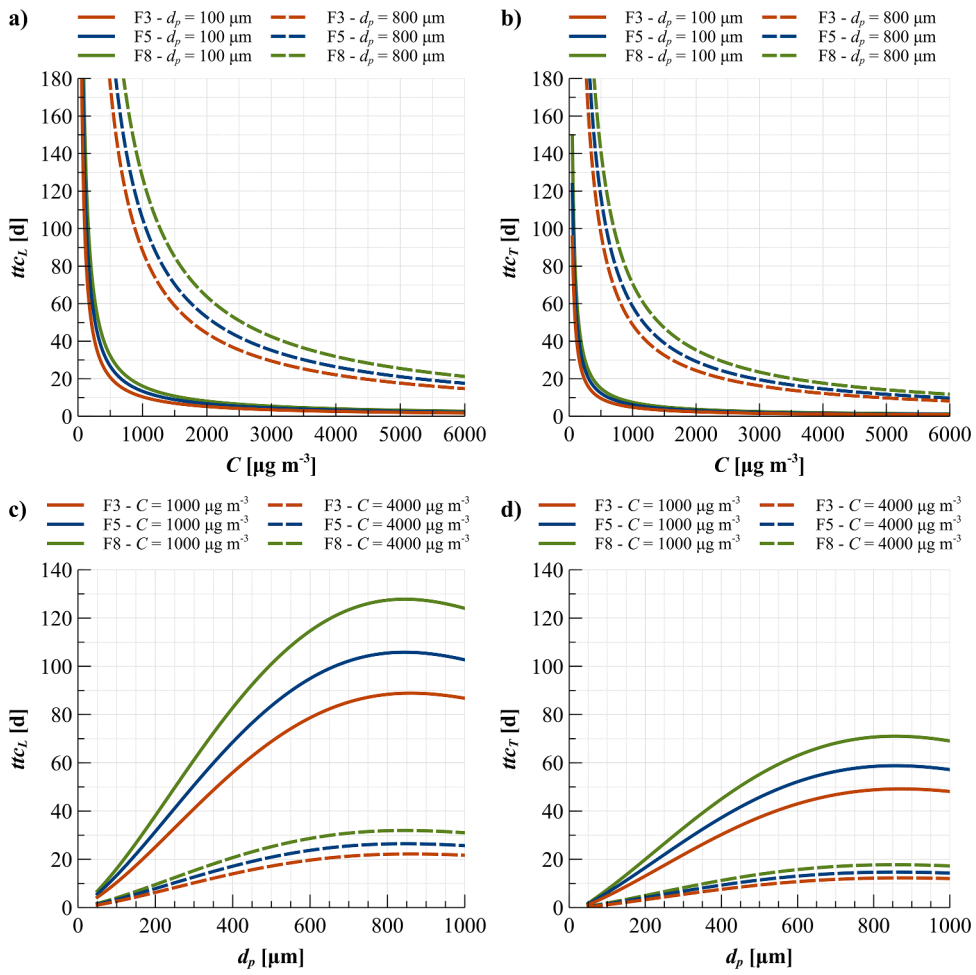

Fig. 15. Time to clogging as a function of the ash particle concentration and particle diameter calculated considering: (a) variable ash particle concentration, loosely correlation, particle diameters of 100 µm and 800 µm; (b) variable ash particle concentration, tapped correlation, particle diameters of 100 µm and 800 µm; (c) variable ash particle diameters, loosely correlation, particle concentration values of 1000 µg•m^{-3} and 4000 µg•m^{-3}; (d) variable ash particle diameter, tapped correlation, concentration values of 1000 µg•m^{-3} and 4000 µg•m^{-3}.

obtained, with potentially severe consequences such as the inability to safely complete the emergency shutdown and the possible development of indirect Natech scenarios caused by the unavailability of utility systems. In Scenarios 3 and 6, it is therefore crucial to carry out a detailed assessment of the potential consequences due to the clogging of filtration systems exposed to volcanic ashes and/or to consider the installation of mitigation measures aimed at increasing the availability of process and instrument air intake systems.

For the medium and high vulnerability scenarios by the screening matrix, Step 4 is applied (see Section 2.6). The results are reported in Fig. 18 for Scenarios 2, 3, 4, and 6, each associated with a different *VVI* value according to the matrix in Fig. 17. Scenario 5 is not shown for the sake of brevity, as it falls into the same vulnerability class as Scenario 4.

As shown in Fig. 18, the probability of clogging never reaches unity in Scenarios 2 and 6. This occurs because the exposure scenario does not always cause filter clogging under loosely packed conditions, in line with the medium level classification in the *VAE* index for these scenarios. Conversely, both loosely and tapped bed clogging is possible in Scenarios 3 and 4.

The results reported in Fig. 18 allow the estimation of the probabilities of accident/near miss, unsafe process shutdown, and safe operation as a function of the duration of the exposure scenario. As shown in the figure, in the case of Scenario 2, the probability of clogging at the completion time of the emergency shutdown is always lower than 0.11, indicating a limited likelihood of accidents and near misses, while the probability of unsafe shutdown (probability that time to clogging is between the time for emergency shutdown and time for process shutdown) equals 0.5. The situation is different for Scenarios 3 and 4, where the probability of accident/near miss is as high as 0.93 and 0.38, respectively. Finally, the probability of clogging has already reached its maximum (about 0.6) before the time at which shutdown is completed in Scenario 6, considering both emergency process procedures.

5. Discussion

A preventive maintenance approach is conventionally applied to air filtration systems, based on monitoring, periodic inspection, testing, and replacement based on recommended operating limits to ensure compliance with standards and process specifications [79,80]. When filters are embedded in safety-critical systems, their failure is considered within general hazard-identification methods (e.g., Hazard and Operability analysis), and protective systems are provided to mitigate the consequences. However, to date, no specific method is applied in current industrial practice to assess the vulnerability of filters in case anomalous concentrations of solid particles are present for a prolonged time. Documented volcanic ash scenarios evidenced the vulnerability of filtration systems exposed to extreme environmental conditions. For example, during the 2011 Cordón Caulle volcanic complex eruption, air intakes, including backup generator intakes, were clogged at two thermal generation facilities, causing power outages in several areas [45].

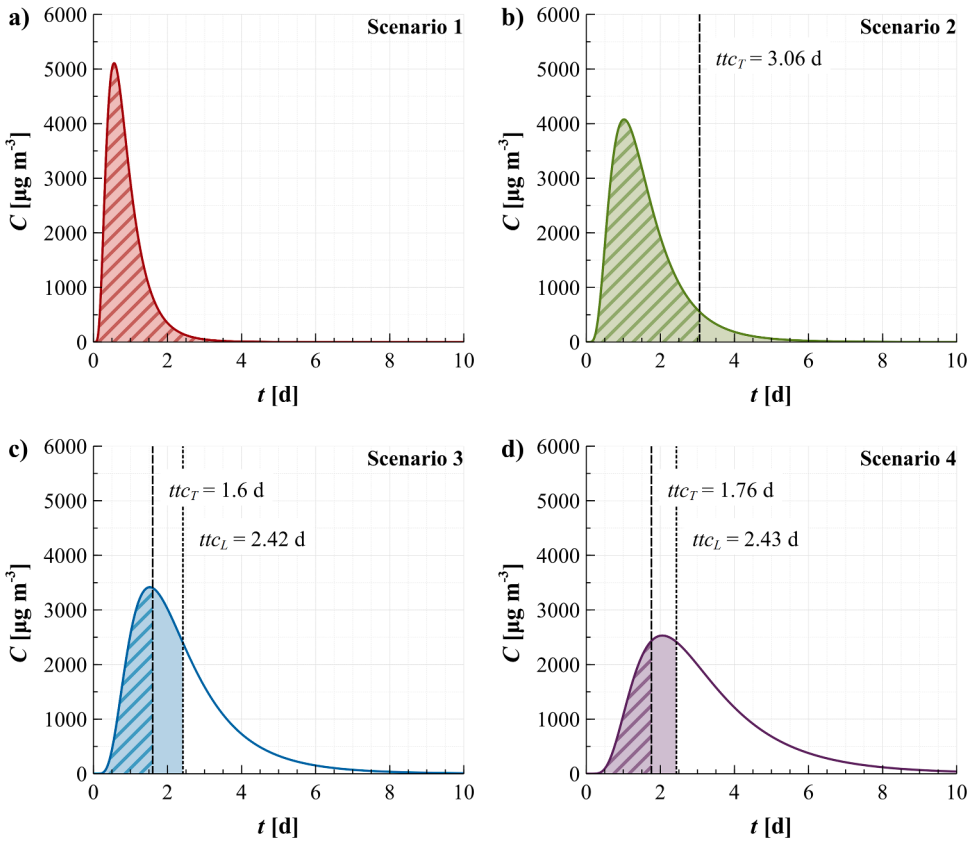

Fig. 16. Concentration vs. time of ash particles and time to clogging of the filtration system for Scenarios 1 to 4 in Test Bed 2 (see Table 10): (a) Scenario 1; (b) Scenario 2; (c) Scenario 3; (d) Scenario 4. Solid filling shows the results obtained considering the loosely packing correlation (ttc_L). Striped filling shows the results obtained considering the tapped packing case (ttc_T).

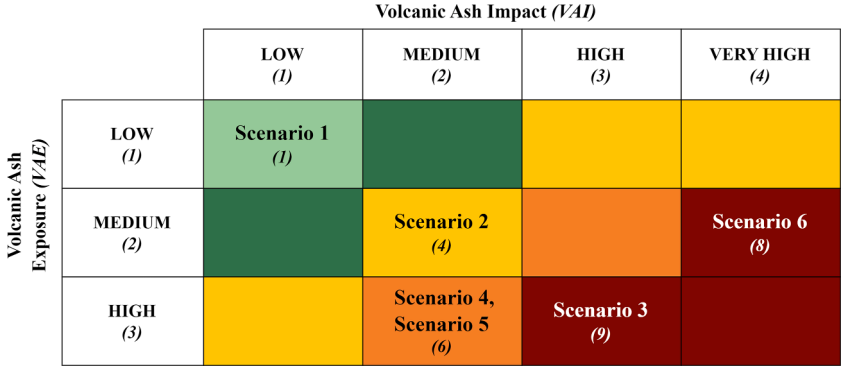

Fig. 17. Results of the vulnerability ranking for the scenarios considered in Test Bed 2.

These observations suggest that an approach only based on programmed and "on-demand" maintenance is insufficient to prevent business interruptions and/or Natech scenarios in case of extreme events, requiring a targeted identification of ash-critical systems.

The original approach developed in the present study provides a method to screen the hazard due to volcanic ash fallout and to identify critical equipment, thus providing a novel tool allowing a systematic screening of the potential hazard generated by volcanic ash fallout on exposed sites. The results also allow the identification of candidate equipment for follow-up quantitative studies. For these systems, the methodology developed is used to quantify the risk associated to the filter clogging, which can be directly integrated into existing Natech risk assessment methods, supporting the implementation of a structured approach to prevent Natech scenarios caused by volcanic ash intake in air supply systems.

The generalized model for filter clogging by volcanic ash developed in the present study accounts for the variability and uncertainty in the filter characteristics, ash properties, cake packing conditions, and the remaining lifetime of the filter. The surrogate model derived from the detailed approach, enabling a more streamlined assessment of the time to clogging that relies on fewer input parameters, provides a robust method for *ttc* evaluation suitable for a preliminary assessment of filter vulnerability in the early stages of eruption scenarios, when a detailed characterization of volcanic ash is not yet available.

The model developed was combined with a scenario-specific vulnerability matrix in order to identify critical equipment, screening the vulnerability to volcanic ash of process and instrument air intake systems. The matrix is based on a quantitative evaluation of volcanic ash

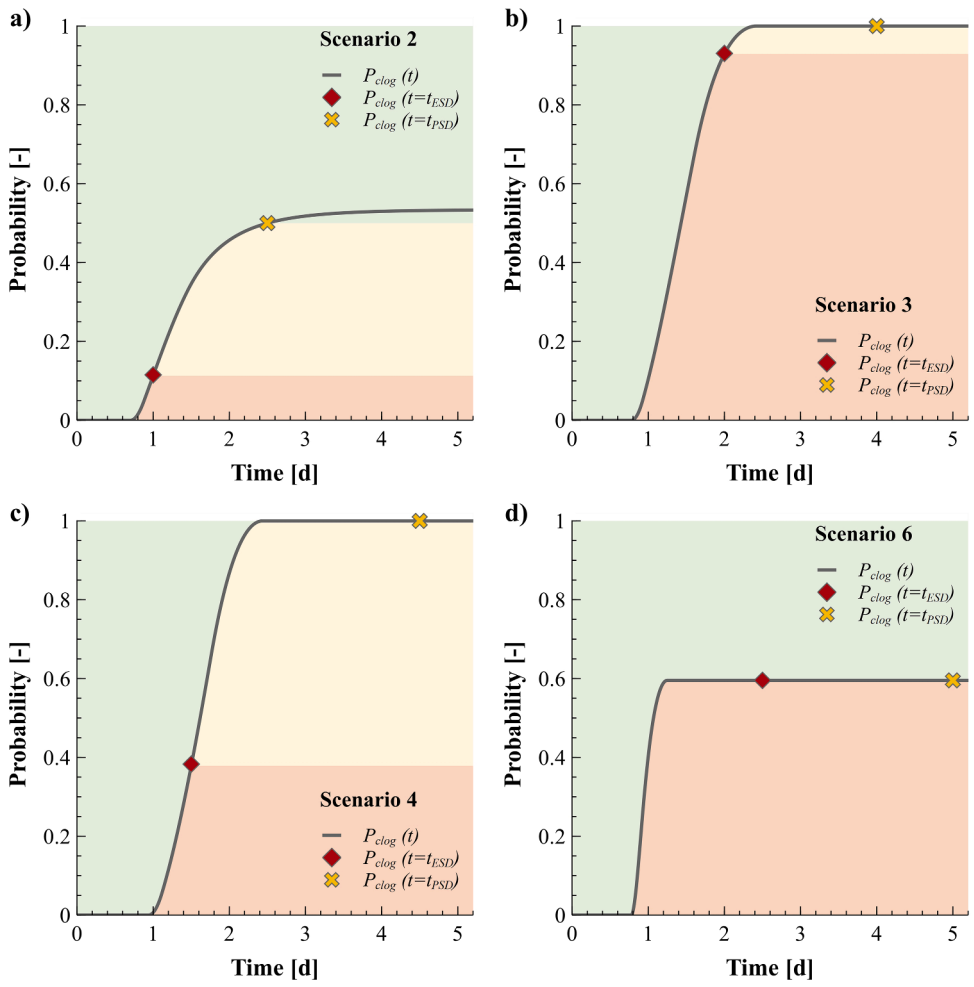

Fig. 18. Clogging probability as a function of time and comparison with time for completion of emergency and process shutdown for (a) Scenario 2, (b) Scenario 3, (c) Scenario 4, and (d) Scenario 6 defined in Test Bed 2.

exposure and impact for a specific scenario, allowing a robust vulnerability ranking of process and instrument air intake systems in the case of exposure to volcanic ash clouds. This effectively supports screening methodologies in identifying equipment items or sites requiring a detailed risk assessment or the introduction of mitigation measures to increase the availability of air intake systems, without imposing unnecessary burden on routine risk management processes. Even if the matrix developed provides a simplified semi-quantitative approach, it is widely recognized as an adequate tool to support decision-making and to strengthen plant-level operational safety, especially in emergency management contexts that require rapid response. Although specifically developed for open-air filtration systems, the matrix can also be applied to other natural hazards causing high concentrations of particulate in air, for example, wildfire ash [81] and sand/dust storms [82].

As a follow-up to the matrix, a Monte Carlo-based model has been developed to quantify the risk due to filter clogging as a function of time for the vulnerable systems identified by the screening approach. The resulting time-dependent clogging probability curves can be used to identify operational regions with distinct safety implications. In addition, clogging probabilities can be directly integrated into existing Natech risk assessment frameworks, allowing the extension of the multi-hazard assessment of Natech scenarios to the scenarios arising from volcanic ash. Clearly enough, alternative approaches can be developed to further extend the risk assessment and management related to volcanic ash within a QRA framework. Options include, among others, Bayesian Network methods, dynamic approaches, or methodologies based on demand and capacity modelling, widely applied in similar contexts [14,83-86].

The application of the novel methodology developed to Test Bed 1 provided relevant information concerning the vulnerability of the different categories of filters to volcanic ash. In particular, coarse filters (i.e., class G) resulted in the more vulnerable category to clogging, followed by medium filters (i.e., class M) and fine filters (i.e., class F). This derives from the features of the filtration systems belonging to the different categories considered, with coarse filters typically having modest allowable maximum pressure drops and lower ratios between the filtration area and the intake area. However, it should be remarked that in most industrial applications, filters are combined in high-performance multilayer filtration systems, with coarse filter panels typically serving as the first filtration layer in contact with the intake air [87]. Since the vulnerability to clogging mostly depends on the characteristics of the first filtration panel, multilayer filtration systems may show a specific vulnerability to volcanic ash exposure.

The results of the assessment of the scenarios included in Test Bed 2, based on realistic data for particle concentration and diameter at different distances from an eruption site, evidence that the hazard caused by volcanic ashes is not specifically dependent on the distance from the eruption site. On the contrary, the data obtained from actual eruptions show that the hazard initially increases with distance. This results from the deposition of the particles with larger diameters, which significantly decreases the airborne concentration with distance, causing the formation of cakes of smaller particles with higher specific pressure drops. This initially offsets the effect of the decrease in ash concentration, causing a decrease in the *ttc*.

The results show that the models developed for the time to clogging of filtration systems allow a thorough characterization of the vulnerability of critical utilities to volcanic ashes. In order to predict the time to clogging, both the detailed and the surrogate models consider two extreme conditions of the void fraction of the filter cake (loosely packing and tapped packing, see Sections 2.3.2 and 2.4.2), thus providing a credible time range for filter clogging. In applications where a single representative *ttc* is required, the adoption of the value corresponding to the tapped packing condition is suggested, since continuous airflow and vibrations induced by the blowers cause particle movements and reduce the cake void fraction. The tapped value of the *ttc* thus represents both the more representative condition for plant operation and the worst-case scenario, providing a conservative basis for decision-making on the safe side.

The overall approach developed may also be applied to real-time assessments during an ongoing volcanic event. In case specific information is available from a volcanic observatory (e.g., an alert for volcanic activity is issued [88]) and a volcanic ash forecast is provided, the *ttc* and specific scenario vulnerability can be assessed, providing a rapid but technically sound assessment of time to clogging that may support decision-making at the site, aiming at preventing indirect Natech scenarios and at minimizing downtime periods and economic losses. The application of the developed methodology can significantly enhance the resilience of industrial installations by improving monitoring and anticipatory capabilities through an engineered approach. The evaluation of the time to clogging and volcanic ash vulnerability includes all the characteristics of effective monitoring indicators (e.g., objective, quantitative, and available [89]), suitable to detect early signs of changing conditions.

6. Conclusions

An innovative methodology was developed to calculate the time to clogging of filtration systems exposed to volcanic ash. The methodology has been integrated into a quantitative approach to assess the scenario-specific vulnerability of industrial air intake systems and the risk associated to filter clogging. The results obtained show that the time to clogging of industrial filters exposed to volcanic ash may vary from a few hours to several days, depending on filter characteristics and the exposure scenario. In this sense, test bed 1 resulted in a time to clogging ranging from 6 h to over 1 month. Moreover, the more critical effects are not monotonically decreasing with the distance from the eruption site. Actually, the decrease in particle concentration is more than compensated by the higher specific pressure drops caused by filter cakes formed by smaller particles up to relevant distances from the site of the eruption. This is evident comparing scenario 1 and 3 in test bed 2, where the increase in the distance led the volcanic ash vulnerability index to move from very low ($VVI = 1$) to very high ($VVI = 9$), the latter featuring a probability of 0.93 to evolve into an accident/near miss. Therefore, the results obtained highlight the importance of a specific screening of the hazards due to volcanic ashes for industrial sites potentially affected by volcanic ash clouds. Overall, the approach developed provides a comprehensive tool for vulnerability screening and assessment of the risk associated to volcanic ash fallout scenarios, supporting both Natech risk assessment studies and the real-time screening of the hazard posed by specific exposure scenarios.

CRediT authorship contribution statement

Matteo Valente: Writing – original draft, Visualization, Investigation, Data curation. **Federica Ricci:** Writing – review & editing, Methodology, Formal analysis, Conceptualization. **Valerio Cozzani:** Writing – review & editing, Supervision, Methodology, Conceptualization.

Declaration of competing interest

The authors declare that they have no known competing financial interests or personal relationships that could have appeared to influence the work reported in this paper.

Supplementary materials

Supplementary material associated with this article can be found, in the online version, at doi:10.1016/j.ress.2025.112155.

Data availability

Data will be made available on request.

References

[1] Misuri A, Cozzani V. A roadmap for the comprehensive assessment of natech risk - Management and control of technological accidents triggered by natural hazards in the framework of climate change. Elsevier; 2024. https://doi.org/10.1016/B978-0-443-15390-7.00008-X.
[2] Krausmann E, Cruz AM, Salzano E. Natech risk assessment and management. reducing the risk of natural-hazard impact on hazardous installations. Elsevier Inc.; 2017.
[3] Suarez-Paba M.C., Tzioutzios D., Cruz A.M., Krausmann E. Toward Natech Resilient Industries, 2020, p. 45–64. https://doi.org/10.1007/978-981-15-4320-3_4.
[4] Valente M, Ricci F, Cozzani V. A systematic review of Resilience Engineering applications to Natech accidents in the chemical and process industry. Reliab Eng Syst Saf 2025;255:110670. https://doi.org/10.1016/j.ress.2024.110670.
[5] Misuri A, Cozzani V. A paradigm shift in the assessment of Natech scenarios in chemical and process facilities. Process Safety and Environmental Protection 2021; 152:338–51. https://doi.org/10.1016/j.psep.2021.06.018.
[6] OECD, European Union. Managing risks from natural hazards to hazardous installations (Natech): a guide for senior leaders in industry and public authorities. Paris: 2024.
[7] Necci A., Krausmann E. Natech risk management - Guidance for operators of hazardous industrial sites and for national authorities, EUR 31122 EN, JRC129450. Luxembourg: 2022. https://doi.org/10.2760/666413.
[8] Ricci F, Casson Moreno V, Cozzani V. Natech accidents triggered by cold waves. Process Safety and Environmental Protection 2023;173:106–19. https://doi.org/10.1016/j.psep.2023.03.022.
[9] Core Writing Team Calvin K, Dasgupta D, Krinner G, Mukherji A, Thorne PW, Trisos C, et al. IPCC, 2023: climate Change 2023: synthesis Report. In: Lee H, Romero J, editors. Contribution of working groups I, ii and iii to the sixth assessment report of the intergovernmental panel on climate change. Geneva, Switzerland: IPCC; 2023. https://doi.org/10.59327/IPCC/AR6-9789291691647. Core Writing Team.
[10] Ricci F, Casson Moreno V, Cozzani V. A comprehensive analysis of the occurrence of Natech events in the process industry. Process Safety and Environmental Protection 2021;147:703–13. https://doi.org/10.1016/j.psep.2020.12.031.
[11] Cozzani V, Antonioni G, Landucci G, Tugnoli A, Bonvicini S, Spadoni G. Quantitative assessment of domino and NaTech scenarios in complex industrial areas. J Loss Prev Process Ind 2014;28:10–22. https://doi.org/10.1016/j.jlp.2013.07.009.
[12] Misuri A, Ricci F, Sorichetti R, Cozzani V. The effect of safety barrier degradation on the severity of primary natech scenarios. Reliab Eng Syst Saf 2023;235:109272. https://doi.org/10.1016/j.ress.2023.109272.
[13] Misuri A, Landucci G, Cozzani V. Assessment of risk modification due to safety barrier performance degradation in Natech events. Reliab Eng Syst Saf 2021;212: 107634. https://doi.org/10.1016/j.ress.2021.107634.
[14] Ricci F, Misuri A, Scarponi GE, Cozzani V, Demichela M. Vulnerability assessment of industrial sites to interface fires and wildfires. Reliab Eng Syst Saf 2024;243: 109895. https://doi.org/10.1016/j.ress.2023.109895.
[15] Amaducci F, Misuri A, Bonvicini S, Salzano E, Cozzani V. Quantitative risk assessment of Natech scenarios triggered by earthquakes involving pipelines. Reliab Eng Syst Saf 2024;245:109993. https://doi.org/10.1016/j.ress.2024.109993.
[16] Fabbrocino G, Iervolino I, Orlando F, Salzano E. Quantitative risk analysis of oil storage facilities in seismic areas. J Hazard Mater 2005;123:61–9. https://doi.org/10.1016/j.jhazmat.2005.04.015.
[17] Zuluaga Mayorga S, Sánchez-Silva M, Ramírez Olivar OJ, Muñoz Giraldo F. Development of parametric fragility curves for storage tanks: a Natech approach. Reliab Eng Syst Saf 2019;189:1–10. https://doi.org/10.1016/j.ress.2019.04.008.
[18] Antonioni G, Landucci G, Necci A, Gheorghiu D, Cozzani V. Quantitative assessment of risk due to NaTech scenarios caused by floods. Reliab Eng Syst Saf 2015;142:334–45. https://doi.org/10.1016/j.ress.2015.05.020.
[19] Khakzad N, Van Gelder P. Fragility assessment of chemical storage tanks subject to floods. Process Safety and Environmental Protection 2017;111:75–84. https://doi.org/10.1016/j.psep.2017.06.012.

[20] Olivar OJR, Mayorga SZ, Giraldo FM, Sánchez-Silva M, Pinelli J-P, Salzano E. The effects of extreme winds on atmospheric storage tanks. Reliab Eng Syst Saf 2020; 195:106686. https://doi.org/10.1016/j.ress.2019.106686.

[21] Ricci F, Casson Moreno V, Cozzani V. Natech accidents triggered by cold waves. Process Safety and Environmental Protection 2023;173:106–19. https://doi.org/10.1016/j.psep.2023.03.022.

[22] Misuri A, Cozzani V. An innovative framework for chemical and process facilities to support a comprehensive Natech risk assessment. Chem Eng Trans 2022;90: 175–80. https://doi.org/10.3303/CET2290030.

[23] U.S. Chemical Safety and Hazard Investigation Board. Investigation Report. Organic peroxide decomposition, release, and fire at arkema crosby following hurricane harvey flooding. Report Number 2017-08-I-TX. Crosby, TX: 2018.

[24] Tokyo Electric Power Company Inc, Tokyo Electric Power Company Incorporated. Fukushima nuclear accident analysis report. Press Corp. Ltd; 2012.

[25] Joint Research Centre, Gkoktsi K. Probabilistic natech risk analysis in the defence sector. Publications Office of the European Union; 2025. https://doi.org/10.2760/8504832.

[26] Necci A, Krausmann E. Natech risk management - Guidance for operators of hazardous industrial sites and for national authorities, eur 31122 en. Publications Office of the European Union; 2022. https://doi.org/10.2760/666413.

[27] International Atomic Energy Agency (IAEA). Volcanic hazard assessments for nuclear installations: methods and examples in site evaluation. Vienna: IAEA-TECDOC-1795; 2016.

[28] International Atomic Energy Agency (IAEA). Volcanic hazards in site evaluation for nuclear installations: specific safety guide. Vienna: IAEA Safety Standards Series No. SSG-21; 2012.

[29] Loughlin SC, Sparks S, Brown SK, Jenkins SF. Vye-Brown C. global volcanic hazards and risk. Cambridge: Cambridge University Press; 2015. https://doi.org/10.1017/CBO9781316276273.

[30] Wilson TM, Jenkins S, Stewart C. Impacts from volcanic ash fall. volcanic hazards, risks and disasters. Elsevier; 2015. p. 47–86. https://doi.org/10.1016/B978-0-12-396453-3.00003-4.

[31] Brown SK, Loughlin SC, Sparks RSJ, Vye-Brown C. Global volcanic hazards and risk: technical background paper for the global assessment report on disaster risk reduction 2015. Global Volcano Model and IAVCEI,; 2015. p. 1–233.

[32] Reichardt U, Ulfarsson GF, Pétursdóttir G. Volcanic ash and aviation: recommendations to improve preparedness for extreme events. Transp Res Part A Policy Pract 2018;113:101–13. https://doi.org/10.1016/j.tra.2018.03.024.

[33] Takebayashi M, Onishi M, Tobita K, Iguchi M. Impact of volcanic eruptions on flight routing. Case Stud Transp Policy 2025;20:101432. https://doi.org/10.1016/j.cstp.2025.101432.

[34] Salzano E, Basco A. A preliminary analysis of volcanic Na-tech risks in the Vesuvius Area. editors. In: Martorell S, Guedes Soares C, Barnett J, editors. Safety, reliability and risk analysis: theory, methods and applications. London: CRC Press, Taylor & Francis; 2009. p. 3085–92.

[35] Milazzo MF, Ancione G, Basco A, Lister DG, Salzano E, Maschio G. Potential loading damage to industrial storage tanks due to volcanic ash fallout. Natural Hazards 2013;66:939–53. https://doi.org/10.1007/s11069-012-0518-5.

[36] Milazzo MF, Primerano P, Ancione G, Salzano E, Maschio G. Potential damages of atmospheric storage tanks due to volcanic ash aggregations in presence of water. Chem Eng Trans 2014;36:487–92. https://doi.org/10.3303/CET1436082.

[37] Milazzo MF, Ancione G, Lister DG, Basco A, Salzano E, Maschio G. Analysis of the effects due to Ash fallout from Mt. Etna on industrial installations. Chem Eng Trans 2012;26:123–8. https://doi.org/10.3303/CET1226021.

[38] Wardman JB, Wilson TM, Bodger PS, Cole JW, Stewart C. Potential impacts from tephra fall to electric power systems: a review and mitigation strategies. Bull Volcanol 2012;74:2221–41. https://doi.org/10.1007/s00445-012-0664-3.

[39] Ancione G, Salzano E, Maschio G, Milazzo MF. Vulnerability of wastewater treatment plants to volcanic Na-tech events. Chem Eng Trans 2014;36:433–8. https://doi.org/10.3303/CET1436073.

[40] Ancione G, Salzano E, Maschio G, Milazzo MF. A GIS-based tool for the management of industrial accidents triggered by volcanic ash fallouts. J Risk Res 2016;19:212–32. https://doi.org/10.1080/13669877.2014.961515.

[41] Wilson TM, Stewart C, Sword-Daniels V, Leonard GS, Johnston DM, Cole JW, et al. Volcanic ash impacts on critical infrastructure. Physics and Chemistry of the Earth 2012;45-46:5–23. https://doi.org/10.1016/j.pce.2011.06.006. Parts A/B/C.

[42] Wilson G, Wilson TM, Deligne NI, Cole JW. Volcanic hazard impacts to critical infrastructure: a review. Journal of Volcanology and Geothermal Research 2014; 286:148–82. https://doi.org/10.1016/j.jvolgeores.2014.08.030.

[43] McDuffie S, Diaz E. Mitigating volcanic ashfall at a high-level wate treatment facility. In: 23rd Conference on Structural Mechanics in Reactor Technology (SMiRT-23); 2015.

[44] Takanaga K., Kurahashi Y., Takemoto J., Ikeda Y., Saito K. Efforts to support for restarting BWR plants. 2025.

[45] Craig H, Wilson T, Stewart C, Outes V, Villarosa G, Baxter P. Impacts to agriculture and critical infrastructure in Argentina after ashfall from the 2011 eruption of the Cordón Caulle volcanic complex: an assessment of published damage and function thresholds. Journal of Applied Volcanology 2016;5:7. https://doi.org/10.1186/s13617-016-0046-1.

[46] Milazzo MF, Ancione G, Salzano E, Maschio G. Risks associated with volcanic ash fallout from Mt.Etna with reference to industrial filtration systems. Reliab Eng Syst Saf 2013;120:106–10. https://doi.org/10.1016/j.ress.2013.05.008.

[47] Milazzo MF, Ancione G, Salzano E, Lister DG, Maschio G. Potential damage to filtration systems due to volcanic ash fallout. In: 11th International Probabilistic Safety Assessment and Management Conference and the Annual European Safety and Reliability Conference 2012 (PSAM11 ESREL 2012). Curran Associates, Inc.; 2012. p. 5379–87.

[48] Ergun S. Flow through packed columns. Chem Eng Prog 1952;48.

[49] Hoffmann AC, Finkers HJ. A relation for the void fraction of randomly packed particle beds. Powder Technol 1995;82:197–203. https://doi.org/10.1016/0032-5910(94)02910-G.

[50] Li Q, Wang Z, Shao S, Niu Z, Xin Y, Zhao D, et al. Experimental study on the synthetic dust loading characteristics of air filters. Sep Purif Technol 2022;284: 120209. https://doi.org/10.1016/j.seppur.2021.120209.

[51] Wang Q, Lin X, Chen D-R. Effect of dust loading rate on the loading characteristics of high efficiency filter media. Powder Technol 2016;287:20–8. https://doi.org/10.1016/j.powtec.2015.09.032.

[52] Green DW, Perry RH. Perry's chemical engineers' handbook. 8th edition. McGraw-Hill; 2008. https://doi.org/10.1036/0071422943.

[53] Scollo S, Tarantola S, Bonadonna C, Coltelli M, Saltelli A. Sensitivity analysis and uncertainty estimation for tephra dispersal models. J Geophys Res Solid Earth 2008;113. https://doi.org/10.1029/2006JB004864.

[54] Scollo S, Del Carlo P, Coltelli M. Tephra fallout of 2001 Etna flank eruption: analysis of the deposit and plume dispersion. Journal of Volcanology and Geothermal Research 2007;160:147–64. https://doi.org/10.1016/j.jvolgeores.2006.09.007.

[55] Bonadonna C, Phillips JC. Sedimentation from strong volcanic plumes. J Geophys Res Solid Earth 2003;108. https://doi.org/10.1029/2002JB002034.

[56] Pardini F, Spanu A, de' Michieli Vitturi M, Salvetti MV, Neri A. Grain size distribution uncertainty quantification in volcanic ash dispersal and deposition from weak plumes. J Geophys Res Solid Earth 2016;121:538–57. https://doi.org/10.1002/2015JB012536.

[57] Bagheri GH, Bonadonna C, Manzella I, Vonlanthen P. On the characterization of size and shape of irregular particles. Powder Technol 2015;270:141–53. https://doi.org/10.1016/j.powtec.2014.10.015.

[58] INTERNATIONAL CIVIL AVIATION ORGANIZATION. VOLCANIC ash contingency plan afi region. 2011.

[59] Saltelli A, Tarantola S, Campolongo F, Ratto M. Sensitivity analysis in practice. Wiley; 2002. https://doi.org/10.1002/0470870958.

[60] Morris MD. Factorial sampling plans for preliminary computational experiments. Technometrics 1991;33:161. https://doi.org/10.2307/1269043.

[61] Ye M, Hill MC. Global sensitivity analysis for uncertain parameters, models, and scenarios. Sensitivity analysis in earth observation modelling. Elsevier; 2017. p. 177–210. https://doi.org/10.1016/B978-0-12-803011-0.00010-0.

[62] Freudenberg Filtration Technologies SE & Co. KG. Viledon - HYDROMAXX Reverse pocket filters. 2018. https://tricanfiltration.com/wp-content/uploads/2021/06/Viledon-HydroMaxx-Reverse-Pocket-Filters.pdf (accessed September 24, 2024).

[63] Freudenberg Filtration Technologies SE & Co. KG. Viledon - T90 And T90 PRE compact pocket filters. 2021. https://menardifilters.se/wp-content/uploads/T90_T90PRE_Turbo_DS_02-CC-026-January-2021-EN.pdf (accessed September 24, 2024).

[64] Klawonn M, Frazer LN, Wolfe CJ, Houghton BF, Rosenberg MD. Constraining particle size-dependent plume sedimentation from the 17 June 1996 eruption of Ruapehu Volcano, New Zealand, using geophysical inversions. J Geophys Res Solid Earth 2014;119:1749–63. https://doi.org/10.1002/2013JB010387.

[65] Nicotra G, Rossi E, Decarli L, Di Talia V, Tugnoli A, Cozzani V. Natech (Natural Hazard Triggering Technological Disasters) Events Risk Management: an operational approach. In: SPE International Health, Safety, Environment and Sustainability Conference and Exhibition. SPE; 2024. https://doi.org/10.2118/220492-MS.

[66] Delvosalle C, Fiévez C, Pipart A. Appendix 13: risk Matrix. ARAMIS: Accidental Risk Assessment Methodology for Industries in the context of the Seveso II Directive 2004.

[67] International Organization for Standardization. Petroleum and natural gas industries - Offshore production installations - Major Accident hazard management during the design of new installations (ISO 17776:2016). Geneva, Switzerland: 2016.

[68] Rios Insua D, Alfaro C, Gomez J, Hernandez-Coronado P, Bernal F. A framework for risk management decisions in aviation safety at state level. Reliab Eng Syst Saf 2018;179:74–82. https://doi.org/10.1016/j.ress.2016.12.002.

[69] Marzo E, Busini V, Rota R. Definition of a short-cut methodology for assessing the vulnerability of a territory in natural-technological risk estimation. Reliab Eng Syst Saf 2015;134:92–7. https://doi.org/10.1016/j.ress.2014.07.026.

[70] Misuri A, Casson Moreno V, Quddus N, Cozzani V. Lessons learnt from the impact of hurricane Harvey on the chemical and process industry. Reliab Eng Syst Saf 2019;190:106521. https://doi.org/10.1016/j.ress.2019.106521.

[71] Freudenberg Filtration Technologies SE & Co. KG. Multi-stage filtration solutions for gas turbines and compressors. 2024. https://www.freudenberg-filter.com/en (accessed December 10, 2024).

[72] British Standards Institution. BS en 779-2012: particulate air filters for general ventilation — determination of the filtration performance. London: 2012.

[73] Devenish BJ, Thomson DJ, Marenco F, Leadbetter SJ, Ricketts H, Dacre HF. A study of the arrival over the United Kingdom in April 2010 of the Eyjafjallajökull ash cloud using ground-based lidar and numerical simulations. Atmos Environ 2012; 48:152–64. https://doi.org/10.1016/j.atmosenv.2011.06.033.

[74] Biass S, Scaini C, Bonadonna C, Folch A, Smith K, Höskuldsson A. A multi-scale risk assessment for tephra fallout and airborne concentration from multiple Icelandic volcanoes - part 1: hazard assessment. Natural Hazards and Earth System Sciences 2014;14:2265–87. https://doi.org/10.5194/nhess-14-2265-2014.

[75] Bonadonna C, Phillips JC, Houghton BF. Modeling tephra sedimentation from a Ruapehu weak plume eruption. J Geophys Res Solid Earth 2005;110. https://doi.org/10.1029/2004JB003515.
[76] Harvey NJ, Herzog M, Dacre HF, Webster HN. A comparison of volcanic ash source term characteristics estimated by source inversion and plume rise modelling methods: raikoke 2019. Journal of Volcanology and Geothermal Research 2025; 462:108304. https://doi.org/10.1016/j.jvolgeores.2025.108304.
[77] Bonadonna C, Genco R, Gouhier M, Pistolesi M, Cioni R, Alfano F, et al. Tephra sedimentation during the 2010 Eyjafjallajökull eruption (Iceland) from deposit, radar, and satellite observations. J Geophys Res Solid Earth 2011;116:B12202. https://doi.org/10.1029/2011JB008462.
[78] Met Office. Volcanic ash concentration archive. 2024. https://www.metoffice.gov.uk/services/transport/aviation/regulated/international-aviation/vaac/concentration-charts/archive (accessed December 10, 2024).
[79] Instrument Society of America. Quality standard for instrument air. Research Triangle Park, North Carolina: Instrument Society of America; 1996.
[80] International Organization for Standardization. BS iso 8573-1:2010 - Compressed air - Part 1: contaminants and purity classes. Geneva: 2010.
[81] United States Environmental Protection Agency. Wildfires and indoor air quality. IAQ; 2025. https://www.epa.gov/emergencies-iaq/wildfires-and-indoor-air-quality-iaq (accessed September 23, 2025).
[82] World Health Organization. Sand and dust storms. 2025. https://www.who.int/news-room/fact-sheets/detail/sand-and-dust-storms (accessed September 23, 2025).
[83] Li S-Q, Gardoni P. Optimized seismic hazard and structural vulnerability model considering macroseismic intensity measures. Reliab Eng Syst Saf 2024;252: 110460. https://doi.org/10.1016/j.ress.2024.110460.
[84] Khakzad N, Van Gelder P. Vulnerability of industrial plants to flood-induced natechs: a Bayesian network approach. Reliab Eng Syst Saf 2018;169:403–11. https://doi.org/10.1016/j.ress.2017.09.016.
[85] Zuluaga Mayorga S, Sánchez-Silva M, Ramírez Olivar OJ, Muñoz Giraldo F. Development of parametric fragility curves for storage tanks: a Natech approach. Reliab Eng Syst Saf 2019;189:1–10. https://doi.org/10.1016/j.ress.2019.04.008.
[86] Ricci F, Yang M, Reniers G, Cozzani V. Emergency response in cascading scenarios triggered by natural events. Reliab Eng Syst Saf 2024;243:109820. https://doi.org/10.1016/j.ress.2023.109820.
[87] Sparks T, Chase G. Filters and filtration handbook. Elsevier; 2016. https://doi.org/10.1016/C2012-0-03230-9.
[88] Civil Protection Department Presidency of the Council of Ministers (Italian goverment). Activities - Volcanic risk. 2024. https://rischi.protezionecivile.gov.it/en/volcanic/activities/ (accessed December 12, 2024).
[89] Hollnagel E, Pariès J, Woods DD, Wreathall J. Resilience engineering in practice. CRC Press; 2013. https://doi.org/10.1201/9781317065265.